

UNCLASSIFIED

AD NUMBER

AD227572

LIMITATION CHANGES

TO:

Approved for public release; distribution is unlimited.

FROM:

Distribution authorized to U.S. Gov't. agencies and their contractors;
Administrative/Operational Use; 01 SEP 1959.
Other requests shall be referred to Office of Naval Research, Arlington, VA 22203.

AUTHORITY

ONR ltr 9 Nov 1977

THIS PAGE IS UNCLASSIFIED

THIS REPORT HAS BEEN DELIMITED
AND CLEARED FOR PUBLIC RELEASE
UNDER DOD DIRECTIVE 5200.20 AND
NO RESTRICTIONS ARE IMPOSED UPON
ITS USE AND DISCLOSURE.

DISTRIBUTION STATEMENT A

APPROVED FOR PUBLIC RELEASE;
DISTRIBUTION UNLIMITED.

UNCLASSIFIED

AD

227572

FOR
MICRO-CARD
CONTROL ONLY

1 OF 2

Reproduced by

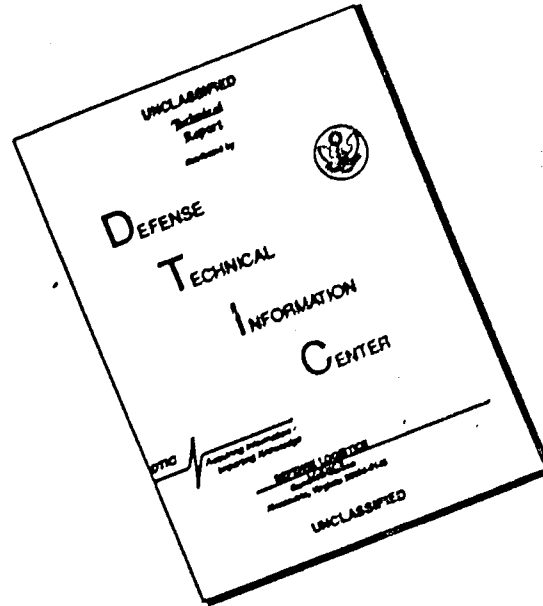
Armed Services Technical Information Agency

ARLINGTON HALL STATION; ARLINGTON 12 VIRGINIA

UNCLASSIFIED

"NOTICE: When Government or other drawings, specifications or other data are used for any purpose other than in connection with a definitely related Government procurement operation, the U.S. Government thereby incurs no responsibility, nor any obligation whatsoever; and the fact that the Government may have formulas furnished, or in any way supplied the said drawings, specifications or other data is not to be regarded by implication or otherwise in any manner licensing the holder or any other person or corporation, or conveying any rights or permission to manufacture, use or sell any patented invention that may in any way be related thereto."

DISCLAIMER NOTICE



THIS DOCUMENT IS BEST QUALITY AVAILABLE. THE COPY FURNISHED TO DTIC CONTAINED A SIGNIFICANT NUMBER OF PAGES WHICH DO NOT REPRODUCE LEGIBLY.

AD No. 227572

ASTIA FILE COPY

THE INFLUENCE OF TEMPERATURE DEPENDENT PROPERTIES ON GAS FLOW HEAT TRANSFER IN CIRCULAR TUBES

BY
W. B. NICOLL AND W. M. KAYS

TECHNICAL REPORT NO. 43

FC

PREPARED UNDER CONTRACT Nonr 275 (23)
(NR-090-342)
FOR
OFFICE OF NAVAL RESEARCH

ASTIA
NOV 8 1959
TIPDR B

DEPARTMENT OF MECHANICAL ENGINEERING
STANFORD UNIVERSITY
STANFORD, CALIFORNIA

SEPTEMBER 1, 1959

FILE COPY
Return to
ASTIA
ARLINGTON HALL STATION
ARLINGTON 12, VIRGINIA
Attn: TISS

THE INFLUENCE OF TEMPERATURE DEPENDENT PROPERTIES
ON GAS FLOW HEAT TRANSFER IN CIRCULAR TUBES

Technical Report No. 43

Prepared under Contract Nonr 225(23)
(NR-090-342)

For
Office of Naval Research

Reproduction in whole or part is permitted for
any purpose of the United States Government

Department of Mechanical Engineering
Stanford University
Stanford, California

September 1, 1959

Report Prepared By:

W. B. Nicoll
W. M. Kays

Approved By:

A. L. London
W. M. Kays
Project Supervisors

ACKNOWLEDGEMENTS

The apparatus for the laminar and turbulent cooling experiments was designed by Mr. Robert I. Jetter, graduate student in Mechanical Engineering. The cooling experiments were in part carried out by Mr. Kerry D. Favro, graduate student in Mechanical Engineering.

ABSTRACT

When convective heat transfer takes place under large temperature difference conditions the fluid transport properties may vary markedly over the flow cross-section, invalidating theoretical solutions based on constant properties and empirical correlations based on small temperature difference experiments. This problem has been investigated analytically for fully established laminar and turbulent flow in circular tubes, but the only really extensive experimental work for the case of the flow of a gas appears to be for turbulent flow with the gas being heated. The analytical solutions indicate that the turbulent flow heating problem shows the greatest temperature dependent properties effect, while the effects are small for laminar heating and negligible for laminar and turbulent cooling, but experimental verification of this fact is meager and some of the simplifying assumptions in the analyses definitely require verification. The objective of the present investigation ^{attempts} ~~has been~~ to experimentally determine the effect of large temperature differences for flow of air in a circular tube under the conditions of laminar flow heating, laminar flow cooling, and turbulent flow cooling.

Experimental data are presented for laminar flow heating and cooling up to absolute temperature ratios of about 1.8, and for turbulent flow cooling for absolute temperature ratios from 1.5 to 2.7. The laminar flow heating data, despite temperature rises of as much as 1100°F , and temperature differences as high as 550°F , show negligible temperature dependent properties effects, and in fact correspond very closely to the Graetz solution (extended) if all properties are evaluated at local mixed-mean temperature. The laminar cooling data also correspond well with the Graetz solution for mean Nusselt number with respect to length, provided that properties are evaluated at the logarithmic mean temperature with respect to end temperatures and wall temperature. The turbulent cooling data show no detectible effect of temperature ratio when properties are evaluated at the logarithmic mean temperature.



TABLE OF CONTENTS

	Page
Acknowledgements	iii
Abstract	iv
Nomenclature	
I. Introduction and objectives.	1
II. Constant property analytical solutions	5
III. Summary of previous work on the influence of temperature dependent gas properties	11
Fig. 1a - Turbulent flow, circular tube - Analysis of Sze and NACA experiments	14
Fig. 1b - Fully developed laminar flow - Analysis of Sze	14
IV. Experimental apparatus	15
Table I - A summary of important apparatus dimensions.	18
Fig. 2 - Air supply and metering system.	19
Fig. 3 - Laminar heating apparatus	19
Fig. 4 - Gas cooling apparatus	20
Fig. 5 - Laminar heating apparatus, thermocouple location	20
V. Reduction of experimental data and test results.	21
Laminar heating experiments	21
Table II - The functions $A(x^+)$ and $B(x^+)$	29
Cooling experiments	29
Analysis of experimental uncertainty.	33
Test results.	33
Fig. 6 - Laminar flow heating, Run 1 - N_{Nu_x} vs x^+	35
Fig. 7 - Laminar flow heating, Run 2 - N_{Nu_x} vs x^+	35
Fig. 8 - Laminar flow heating, Run 3 - N_{Nu_x} vs x^+	36
Fig. 9 - Laminar flow heating, Run 4 - N_{Nu_x} vs x^+	36

TABLE OF CONTENTS (Cont'd)

	Page
Fig. 10 - Laminar flow heating, Run 5 - N_{Nu_x} vs x^+	37
Fig. 11 - Laminar flow heating, Run 6 - N_{Nu_x} vs x^+	37
Fig. 12 - Laminar flow heating, Runs 1, 2, 3, 4, 5, 6 - $N_{Nu_x}/N_{Nu_{iso}}$ vs T_w/T_m	38
Fig. 13 - Laminar cooling, $N_{Nu}/N_{Nu_{iso}}$ vs T_m/T_w - Properties evaluated at log-mean temperature	39
Fig. 14 - Laminar cooling, $N_{Nu}/N_{Nu_{iso}}$ vs T_m/T_w - Properties evaluated at "Graetz mean" temperature	39
Fig. 15 - Laminar cooling, $N_{Nu}/N_{Nu_{iso}}$ vs T_m/T_w - Properties evaluated at exit temperature	39
Fig. 16 - Turbulent cooling, N_{Nu_m} vs N_{Re}	40
Fig. 17 - Turbulent cooling, $N_{Nu}/N_{Nu_{iso}}$ vs T_m/T_w	40
VI. Discussion of test results	41
Laminar heating	41
Laminar cooling	41
Turbulent cooling	43
VII. Conclusions	44
Appendix A - Summary of eigenvalues and constants	46
Appendix B - Summary of experimental data	48
Appendix C - Analysis of experimental uncertainty	54
References	58

NOMENCLATURE

English Letter Symbols

- A - heat transfer area, ft^2
- A - function of x^+ defined by Eq. (26)
- B - function of x^+ defined by Eq. (26)
- C_n - constant in series solution, Eq. (3)
- c_p - specific heat at constant pressure, $\text{Btu}/(\text{lb}^{\circ}\text{F})$
- D - tube diameter, ft
- G - mass velocity, $\text{lbs}/(\text{hrft}^2)$
- G_n - function defined by Eq. (4)
- $H'(-\gamma_m^2)$ - function defined in Eq. (15)
- h - convection heat transfer conductance, $\text{Btu}/(\text{hrft}^2\text{F})$
- I - electrical current, amps
- k - thermal conductivity, $\text{Btu}/(\text{hrft}^2\text{F}/\text{ft})$
- L - tube length, ft
- L - dummy nondimensional tube length variable of same character as x^+
- L - heat leak, Btu/in
- P - power input, Btu/in
- q - heat flux, $\text{Btu}/(\text{hrft}^2)$
- q' - heat transfer rate per unit length, $\text{Btu}/(\text{hrft})$
- q'' - heat flux (same as q), $\text{Btu}/(\text{hrft}^2)$
- R - electrical resistance, ohms
- R_n - eigenfunctions, see Eq. (3)
- r - radial coordinate measured from tube centerline, ft
- r_o - tube radius, ft
- r^+ - nondimensional radial position, r/r_o

- T - temperature, $^{\circ}\text{R}$
- T_o - uniform fluid temperature at beginning of tube, $^{\circ}\text{R}$
- T_w - wall surface temperature, $^{\circ}\text{R}$
- T_m - mixed-mean fluid temperature, $^{\circ}\text{R}$
- t - thickness of tube wall, ft
- U - overall heat transfer conductance, $\text{Btu}/(\text{hrft}^{\circ}\text{F})$
- V - fluid velocity, ft/sec
- w - fluid flow rate, lbs/hr
- x - axial coordinate in tube, ft
- x^+ - nondimensional axial coordinate, $(x/r_o)/(N_{\text{Re}}N_{\text{Pr}})$

Greek Letter Symbols

- α - thermal diffusivity, ft/hr^2
- α - temperature coefficient of electrical resistivity, $1/^{\circ}\text{F}$
- γ_m - eigenvalue defined by Eq. (14)
- ϵ - heat exchanger effectiveness
- ϵ_H - turbulent eddy diffusivity, ft/hr^2
- θ - nondimensional temperature defined by Eq. (2)
- θ_m - nondimensional mixed-mean temperature
- λ_n - eigenvalue defined by Eq. (3)
- μ - coefficient of viscosity, $\text{lbs}/(\text{hrft})$

Nondimensional Groupings

- N_{Nu} - Nusselt number, hD/k
- N_{Nu_x} - local Nusselt number
- N_{Nu_m} - mean Nusselt number with respect to tube length
- $N_{\text{Nu}_{\text{iso}}}$ - Nusselt number based on constant fluid properties, i.e., with temperature difference approaching zero.
- N_{Re} - Reynolds number, DG/μ

- N_{Pr} - Prandtl number, $\mu c_p/k$
- NTU - number of heat transfer units in a heat exchanger, $AU/(wc_p)$
- x^+ - nondimensional tube length parameter, $(x/r_o)/(N_{Re} N_{Pr})$

SECTION I INTRODUCTION AND OBJECTIVES

The question of the influence of temperature-dependent property variations on the heat transfer characteristics of a gas flowing in a circular tube arises whenever the temperature difference for convection becomes more than 100-200°F. Since most convection heat transfer data have been taken from experiments involving small temperature differences (a temperature difference being small if the mass and thermal transport properties, such as viscosity and thermal conductivity, do not vary significantly through the flow), there is little ambiguity involved when this data is correlated by the use of dimensionless parameters involving the mass and thermal transport properties of the fluid. However, the following question arises when applying these data to situations involving large temperature differences: at what temperature should the properties be evaluated; and what influence has a large property variation across the tube?

In the case of small temperature differences this question does not arise because the transport properties are essentially constant, both across the flow cross-section and in the direction of flow.

For large temperature differences, it is usually most convenient to evaluate the local properties at the local mixed-mean temperature. But if the surface conductance is evaluated from experimental correlations constructed with small temperature difference data, and if all transport properties are evaluated at the local mixed-mean temperature, will the actual local surface conductance, in the case of large temperature difference, be higher or lower, and if so how much?

It should be noted here that temperature dependent property variation across the flow cross-section is not the only important variation. Essentially the same questions as were raised about variations across the flow cross-section can be

raised about variations in the direction of the flow. In fact, frequently the two effects cannot be separated, as in the case of intermediate effectiveness heat exchangers. It is to be expected that for low effectiveness heat exchangers the variation across the flow cross-section will be most important, and that for high effectiveness heat exchangers the variation in the flow direction will be more significant.

As the temperature differences encountered in applications have increased, this question of property variation has become more significant. There is a moderate amount of experimental data involving large temperature differences available, and several methods of correlation have been tried with varying degrees of success. A common approach is to evaluate certain or all of the properties which occur in the dimensionless parameters at some temperature intermediate between the mixed-mean temperature and the tube wall temperature, and some at the mixed-mean temperature. In the case of gases this may involve abandonment of the mass flow velocity (G), a useful parameter about which there is no ambiguity.

In the case of convection heat transfer to or from liquids, density and thermal conductivity can usually be treated as constants, as the variation of these properties is usually small. It is thus only the viscosity which varies markedly, and hence the effects of temperature dependent property variation on the heat transfer characteristics are simply the effects of a deformation of the velocity profile. In this case a correlation in which the viscosity is evaluated at an intermediate or "film" temperature, or the use of a wall-viscosity-to-mixed-mean-viscosity ratio as a correction factor is sufficient.

In the case of convection heat transfer to gases the situation is more complex. Not only can viscosity vary markedly across the flow cross-section and in the flow direction, but also the density and the thermal conductivity. In effect, with gases, the momentum and the energy equations are coupled and must be solved simultaneously. It is no longer possible

to easily predict the effects of the variation of the temperature dependent transport properties. As an illustration of this point, and as an illustration of the sensitivity to geometry, the analytical solutions which do exist^{7*} indicate that for laminar flow between parallel plates the surface conductance will increase when large temperature differences are involved in the case of heating, while for laminar flow in circular tubes under similar conditions the surface conductance will decrease. Fortunately, the important transport properties of most gases vary in a similar fashion with temperature, and hence it is to be expected that experimental data obtained with air as the fluid medium would apply to other gases as well.

Most of the experimental data which involves large temperature differences with gases² has been taken from experiments in which air in turbulent flow was heated. This data can be successfully correlated by a correlation of the form,

$$N_{Nu} = \phi(N_{Re}, N_{Pr}) \left(\frac{T_w}{T_m} \right)^a$$

where a is an empirical constant, and where all properties are evaluated at the mixed-mean temperature of the fluid. The areas of greatest need now for experimental data are turbulent flow with the gas being cooled, and laminar flow, both heating and cooling.

The experimental data taken in this work has been carried out to help fill this gap. In particular, the objectives of this work include the following:

1. To experimentally determine the effect of large temperature differences for a gas being heated at approximately constant heat rate per unit of tube length in laminar flow in a circular tube, and to determine if an entry-length solution of the Graetz type (based on constant properties) can be

*Numbers in superscript refer to the references.

used, with suitable modifications if necessary, under large temperature difference conditions. This part of the investigation is concerned with local heat transfer conductances measured along a tube.

2. To experimentally determine the effect of large temperature differences for a gas being cooled with a constant surface temperature in laminar flow in a circular tube. This part of the investigation is concerned with mean heat transfer conductances with respect to tube length.

3. To experimentally determine the effect of large temperature differences for a gas being cooled with a constant surface temperature in turbulent flow in a circular tube. This part of the investigation is concerned with mean heat transfer conductances with respect to tube length.

The following will be divided into six sections. Because of the great utility of the available analytical solutions, and because they are used as a theoretical reference with which to compare the experimental data, the second section summarizes these solutions. The third summarizes and discusses previous investigations of the problem of temperature dependent property variations in gases flowing in circular tubes. The fourth section is a description of the experimental apparatus. The fifth summarizes the data reduction procedure. In the sixth the experimental results are discussed, and the conclusions are summarized in the seventh.

SECTION II

CONSTANT PROPERTY ANALYTICAL SOLUTIONS

In this section a brief summary of the available analytical solutions for heat transfer to a fluid flowing in a circular tube is presented. More detailed information can be found in the given references. All the solutions presented are for the case of constant properties and fully developed velocity profile. Thus they are only expected to apply where the temperature differences involved are small, and where the velocity profile is fully developed at the start of the heating section, or where the Prandtl number is large so that the velocity profile develops very much more rapidly than the temperature profile.

The Graetz solution covers the case of fully established laminar flow (parabolic velocity profile throughout) with a uniform fluid temperature at the point where the wall surface temperature suddenly steps from the fluid temperature to a new temperature and remains constant thereafter. The solution then yields the fluid temperature as a function of a radial position r^+ , and an axial position, x^+ . These results are obtained starting with the differential energy equation.

$$\frac{1}{r} \frac{\partial}{\partial r} \left[r \frac{\partial T}{\partial r} \right] = \frac{V}{\alpha} \frac{\partial T}{\partial x} \quad (1)$$

After introduction of the parabolic velocity distribution, Eq. (1) may be rendered nondimensional as follows:

$$\frac{1}{r^+} \frac{\partial}{\partial r^+} \left[r^+ \frac{\partial \theta}{\partial r^+} \right] = (1 - r^{+2}) \frac{\partial \theta}{\partial x^+} \quad (2)$$

where

$$\theta = \frac{T_w - T}{T_w - T_o} = \theta(x^+, r^+)$$

$$x^+ = \frac{x}{r_o N_{Re} N_{Pr}}$$

$$r^+ = r/r_o$$

The boundary conditions for (2) are

$$\theta(0, r^+) = 1$$

$$\theta(x^+, 1) = 0$$

Equation (2) with the given boundary conditions is an eigenvalue problem, and the solution may be written in the form

$$\theta = \sum_{n=0}^{\infty} C_n R_n(r^+) e^{-\lambda_n^2 x^+} \quad (3)$$

where R_n are the eigenfunctions and λ_n^2 are the corresponding eigenvalues.

With the temperature distribution established the heat flux at any axial position, $q(x^+)$, may be readily computed from the gradient at the wall.

$$q(x^+) = \frac{2k}{r_0} \sum_{n=0}^{\infty} G_n e^{-\lambda_n^2 x^+} (T_w - T_0) \quad (4)$$

where

$$G_n = -\frac{C_n}{2} R_n'(1)$$

Lipkis¹ has computed a large number of the eigenvalues and constants for Eq. (4). Sellars, Tribus, and Klein³ obtained an asymptotic solution which is accurate for large n . The asymptotic expressions for the eigenvalues and constants are,

$$\lambda_n = 4n + 8/3 \quad (5)$$

$$G_n = 1.01276 \lambda_n^{-1/3} \quad (6)$$

The mixed-mean fluid temperature, θ_m , can be evaluated at any x^+ by integrating Eq. (4) with respect to x^+ , and making an energy balance on the flow stream. The result is

$$\theta_m = \delta \sum_{n=0}^{\infty} \frac{G_n e^{-\lambda_n^2 x^+}}{\lambda_n^2} \quad (7)$$

With the heat flux and mixed-mean temperature established at all points, a local heat transfer coefficient and a local

Nusselt number can readily be defined and evaluated.

$$N_{Nu_x} = \frac{\sum_{n=0}^{\infty} G_n e^{-\lambda_n^2 x^+}}{2 \sum_{n=0}^{\infty} \frac{G_n}{-\lambda_n^2} e^{-\lambda_n^2 x^+}} \quad (8)$$

For large x^+ the series are rapidly convergent, and eventually only the terms corresponding to $n = 0$ are significant. Then Eq. (8) reduces to the expression for the asymptotic Nusselt number for a long tube.

$$N_{Nu_{\infty}} = \frac{\lambda_0^2}{2} \quad (9)$$

Using the Graetz step function solution as a base, the method of superposition can now be employed³ to solve two types of variable surface temperature problems: (a) the surface temperature distribution with length is prescribed and it is desired to evaluate heat flux at all points; (b) the heat flux distribution with length is prescribed and it is desired to evaluate the surface temperature at all points.

If the surface temperature variation is prescribed, the heat flux, $q(x^+)$, at any point may be evaluated from

$$q(x^+) = \frac{k}{r_0} \left[\int_0^{x^+} \theta_{r^+}(x^+ - L, 1) \frac{dT_w}{dL} dL + \sum_{i=1}^k \theta_{r^+}(x^+ - L_i, 1) \Delta T_{w_i} \right] \quad (10)$$

where

$$\theta_{r^+} = -2 \sum_{n=0}^{\infty} G_n e^{-\lambda_n^2 (x^+ - L)} \quad (11)$$

L is a dummy variable varying from 0 to x^+ . The integral in Eq. (10) represents the effects of a continuous variation in the surface temperature while the summation accounts for steps or discontinuities. Thus ΔT_{w_i} is the height of the i th step located at L_i .

If the heat flux is prescribed and the wall temperature

is to be solved for, the problem is more complicated. Only the computing equations will be given here. For more detailed information, see reference 3. The computing equations are as follows:

$$T_w - T_o = \frac{r_o}{k} \int_0^{x^+} g(x^+ - L, 1) q(L) dL \quad (12)$$

where $q(L)$ is the prescribed heat flux as a function of the dummy variable L , and the function $g(x^+, 1)$ is given by,

$$g(x^+, 1) = 4 - \sum_{n=0}^{\infty} \frac{e^{-\gamma_m^2 x^+}}{\gamma_m^2 H'(\gamma_m^2)} \quad (13)$$

The values of γ_m^2 are the zeros of the equation,

$$H(s) = 2 \sum_{n=0}^{\infty} \frac{G_n}{s + \lambda_n^2} \quad (14)$$

where s is the Laplace transform variable. $H'(-\gamma_m^2)$ is then computed after differentiating Eq. (14) and substituting values of γ_m^2 .

$$H'(-\gamma_m^2) = -2 \sum_{n=0}^{\infty} \frac{G_n}{(-\gamma_m^2 + \lambda_n^2)^2} \quad (15)$$

In reference 3 the first three terms for evaluation of Eq. (13) have been computed and tabulated. More recently Sparrow and Hallman⁴ have solved this problem directly rather than through a transform of the constant wall temperature problem. They have evaluated the first five eigenvalues (γ_m^2) and have obtained an asymptotic solution for γ_m .

Sleicher and Tribus⁵ treat the turbulent flow counterpart of the Graetz laminar flow solution, i.e., fully established turbulent flow with a step change in surface temperature. The differential equation solved is the same energy equation, Eq. (1), used for the laminar flow problem, the boundary conditions are identical, and the solution can be

put into the same form and nomenclature. The problem is different from the laminar flow problem in that the velocity in Eq. (1) is now the turbulent velocity profile instead of parabolic, and the thermal diffusivity, α , is replaced by $(\alpha + \epsilon_H)$, where ϵ_H is the turbulent eddy diffusivity for heat transfer. The turbulent velocity profile varies with Reynolds number, and the eddy diffusivity is a function of radial position, Reynolds number, and Prandtl number. The problem is thus more complex, and the eigenvalues and constants will be functions of the Reynolds number and Prandtl number. Sleicher and Tribus used empirical data for the velocity profile and an empirically based modification of the Jenkins⁶ analysis for the eddy diffusivity. Their results can be used to solve the turbulent flow problem where the surface temperature is any prescribed function of tube length through the use of Eqs. (10) and (11).

The Sleicher and Tribus results are limited in two respects. First, they are limited to Prandtl numbers equal to or less than unity. From the point of view of the prescribed surface temperature problem, this is not serious, because only at low Prandtl numbers does a variation in surface temperature markedly affect the surface conductance. The second limitation is that only the first three eigenvalues and constants have been evaluated. In some technical problems these are insufficient to evaluate the series which arise. Also, it is not possible to handle the technically important problem where the heat flux is prescribed without higher order eigenvalues and constants. Sparrow, Hallman, and Siegel³ have solved Eq. (1) for turbulent flow in circular tubes for Prandtl numbers of 0.7, 10, and 100 for the case of constant heat rate per unit of tube length.

Kays and Nicoll⁹ demonstrated that a simple extrapolation of the Sleicher and Tribus results could be used to establish the higher order terms (λ_n^2 and G_n) with an accuracy sufficient to evaluate the γ_m^2 and $H'(-\gamma_m^2)$ to an accuracy commensurate with the uncertainty involved in the knowledge of

the turbulent eddy diffusivity at low Prandtl numbers.

The results of all these analyses have been summarized in Appendix A. These solutions are used as the theoretical reference to which to compare the experimental data collected in this work.

SECTION III

SUMMARY OF PREVIOUS WORK ON THE INFLUENCE OF TEMPERATURE DEPENDENT GAS PROPERTIES

A search of the literature indicates that only two attempts have been made to analytically predict the effects of temperature dependent property variations on the heat transfer characteristics for gas flowing in circular tubes. These are the work of Diessler¹⁰ and the work of Sze⁷. Both give essentially the same results. Both authors used essentially the same simplifying assumptions. The basic differences between the two are in the assumptions made about the functional relationship between the properties and temperature. Diessler assumes that both the thermal conductivity and the viscosity vary with the absolute temperature to the 0.68 power,

$$\frac{k}{k_0} = \frac{\mu}{\mu_0} = \left(\frac{T}{T_0}\right)^{0.68}$$

and that the specific heat is constant, i.e., the Prandtl number is constant. Sze used the experimental variation of these properties with temperature for air, and thus it is felt that his results are more pertinent to the experimental results of this work.

Both Sze and Diessler assumed fully established velocity and temperature profiles and constant heat rate per unit length. It is to be expected that the effects of property variation, like the surface conductance, will depend at least to some extent upon the variation of heat flux with length, although this may well be a second order effect.

The calculating procedure used for laminar flow was an iterative procedure in which a velocity profile was assumed and then a temperature profile calculated. Then, using this temperature profile, the variation of viscosity and thermal conductivity with radial position was determined. With the variation of the viscosity with radius a new velocity profile was calculated, and with this velocity profile, and with the variation of thermal conductivity with radial position, a

new temperature profile was calculated. This process was repeated until the results were unchanged.

From the temperature profile and the velocity profile the mixed-mean temperature can be determined. Then, using the defining equation for the surface conductance, and evaluating the thermal conductivity at the mixed-mean temperature, a Nusselt number can be determined.

For turbulent flow essentially the same method was used, although assumptions had to be made about the variation of the eddy diffusivities as a function of radial position.

Sze's results, plotted on Figs. 1a and 1b, can be approximately represented on logarithmic plots by straight lines, indicating that an experimental correlation of the form,

$$N_{Nu} / N_{Nu_{ISO}} = (T_w / T_m)^a$$

should suffice. The idea of a straight-line correlation is actually better substantiated by the only really significant experimental data, also shown on Fig. 12. It will be noted that for turbulent heating the NACA experimental data lie very close to a straight line with $a = -0.575$. The analysis lies very close to the experimental data for T_w / T_m about 1.5, but indicates a less pronounced effect for temperature ratios between 2 and 3. The analysis involved an iterative procedure which lost in precision at higher temperature ratios, and this is believed to possibly be the reason for the higher temperature ratio discrepancy. The experimental accuracy of the NACA data is probably not sufficiently high to warrant three places in the exponent, but $a = -0.5$ corresponds reasonably closely to both analysis and experiment and is recommended as a good approximation for turbulent heating.

For turbulent cooling the effect is evidently considerably less than for heating, and this is also true for laminar flow, and the available laminar boundary layer solutions indicate the same trend. A line for $a = -0.15$ has been drawn on Fig. 1a, but since there are only two points (other than the origin) upon which to base a line, a smaller exponent

could be just as well justified.

For laminar flow there are no experimental data for comparison. Sze's results, Fig. 1b, would indicate a moderate decrease in conductance (or Nusselt number) for heating, and a very small and possibly negligible increase for cooling. It is, of course, the objective of the present work to resolve these uncertainties, since it is felt that it is only for turbulent heating that the problem is well in hand.

Both the work of Sze and that of Diessler are concerned with the variation of properties in the radial direction only. The effects of property variation in the axial direction have apparently not been investigated analytically. It is usually tacitly assumed that property variation in the axial direction has little or no effect on the local heat transfer characteristics. Thus the local surface conductance, for example, is typically evaluated using the local transport properties and temperature ratios. One of the objectives of this work is to help cast some light on the validity of this assumption.

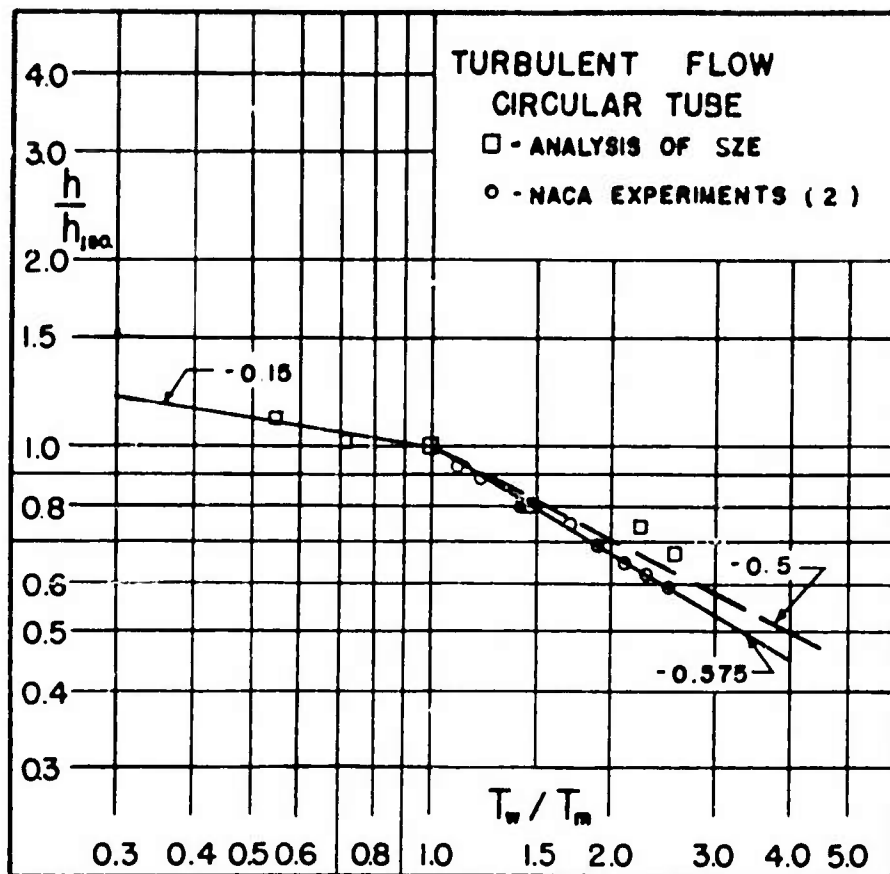


FIG. 1a

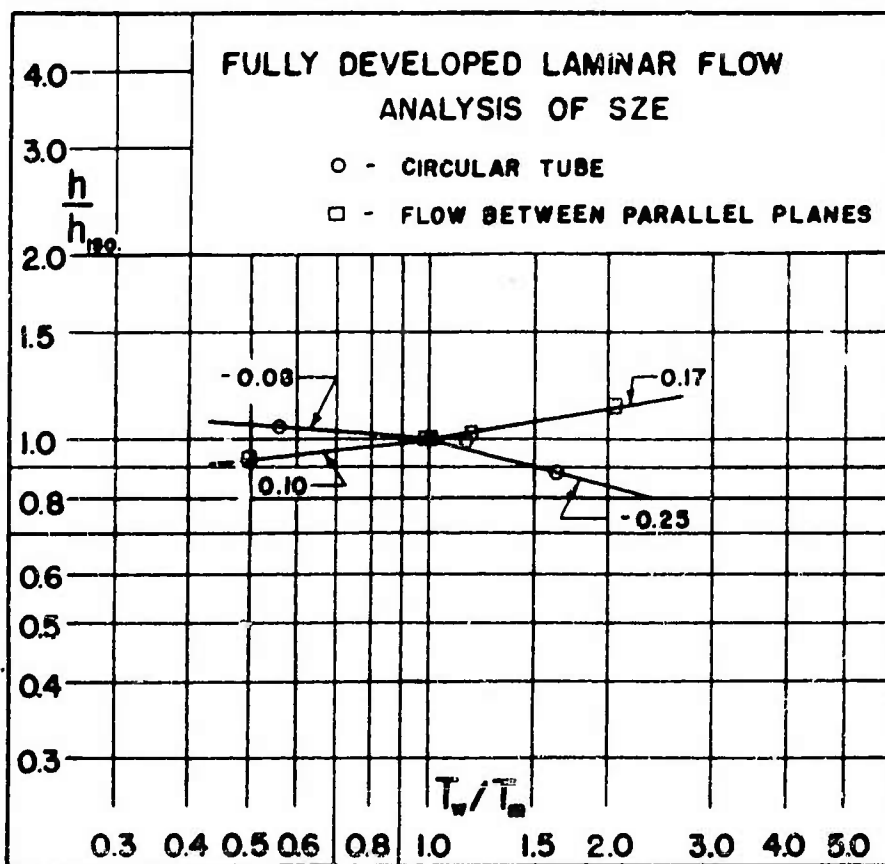


FIG. 1b

SECTION IV EXPERIMENTAL APPARATUS

The experimental apparatus used in this work consists of three elements: 1) an air flow metering and control system; 2) a test section for heating air; and 3) a test section for cooling the air. These elements are shown in Figs. 2, 3, 4, and 5.

The air flow metering system is shown in Fig. 1. The air flow is maintained constant by the use of a series of pressure regulators and valves. The compressor begins operating when the tank pressure falls to 80 psi and cuts out when the pressure reaches 100 psi. A regulator on the outlet of the storage tank further reduces the pressure to 40 psi, and another regulator in series again reduces the pressure to about 10 psi. As the flow rates involved in the laminar flow work are small, it is necessary to bleed off some air between the last pressure regulator and the flow meters. In this way it is possible to completely avoid any detectable variation in the air flow rate.

Two Fischer and Porter Rotameters are used to measure the flow rate, one for the small flows needed for the laminar work, and one for the larger flow rates needed for the turbulent work. Both were carefully calibrated, and the experimental uncertainty is estimated at ± 1 per cent.

The apparatus used for the laminar heating experiments is shown in Figs. 3 and 5. It consists essentially of a 66 inch length of 0.375" OD, 0.005" wall nichrome tube. The first 30 inches are unheated; this section is simply a developing section for the velocity profile. The next 30-inch section is heated by passing an electric current through the tube wall. Thermocouples are spaced along this section for the measurement of the tube wall temperature, Fig. 5. Because of the thinness of the nichrome tube wall, stem conduction in the thermocouples could have been a serious problem. To prevent this as much as possible, the thermocouple

leads are not taken directly away from the tube, but rather are first wound around the tube. The heated section was insulated with Johns-Manville high temperature C11-0-Cel and magnesia sheet insulation.

The point at which heat transfer begins is localized as much as possible by introducing the electric current through a thin flange welded to the tube, as shown in the figures. It is not necessary to know precisely where the heating section ends, and because of this, and because of the high temperatures encountered at the downstream end of the heating section, a simple nichrome collar was fitted to the tube for the attachment of the power leads.

Electric power was supplied to the nichrome tube from a shop-built power-pack constructed from welding transformers, with a variable transformer on the primary for control. The current to the tube was measured using a Weston current transformer and a Weston ammeter. The voltage drop along the tube was measured by a Ballantine vacuum tube voltmeter connected successively to a series of voltage taps welded along the tube.

For purposes of making energy balances, and for checking the calculated fluid mean temperature, a device was fitted to the exit of the nichrome tube for the measurement of the mean air temperature at this point, see Fig. 2. A ceramic tube is fitted over the exit end of the nichrome tube. Short lengths of wire traverse the ceramic tube and serve to mix the air. At the end of this ceramic tube a 1/8" nozzle is fitted to accelerate the flow over the thermocouple. To reduce the heat losses between the end of the heating section and the exit temperature thermocouple, the air was passed back past the ceramic tube before discharging to the atmosphere.

The apparatus for the cooling experiments is somewhat more complicated, and is shown in Fig. 4. From the flow-rater the air flows into a heater, where it is forced through electrically heated nichrome screens. The air then passes through a sharp-edged orifice where it is turbulently mixed.

A thermocouple is situated downstream from this orifice to measure the air temperature. The air then passes into a .500" OD, .010" wall stainless steel tube. The first 32 inches comprise the velocity development section. Because of the low air flow rates involved in the laminar flow experiments, a guard heater of nichrome ribbon is placed around this section for the maintenance of the air temperature. Several thermocouples are attached to the tube wall for checking this temperature.

From the entrance section the air passes through a constant wall temperature section. The wall temperature is maintained constant by passing a large flow of water over the outer surface of the tube in a counter-flow heat exchanger.

The exit air temperature for the laminar flow experiments is measured with the thermocouple system shown in the insert in Fig. 4. A 1/8 inch copper plug is tightly fitted in a balsa-wood sleeve which in turn is tightly fitted inside the nichrome tube just at the end of the cooling section. The copper plug has four equi-spaced No. 58 drill size holes passing through it and a thermocouple attached at its downstream end.

For measuring the exit air temperature during the turbulent flow experiments, where air velocities were substantially higher, a simpler device was used. This consisted of a wire mixer and a 1/8 inch nozzle to accelerate the flow past a thermocouple.

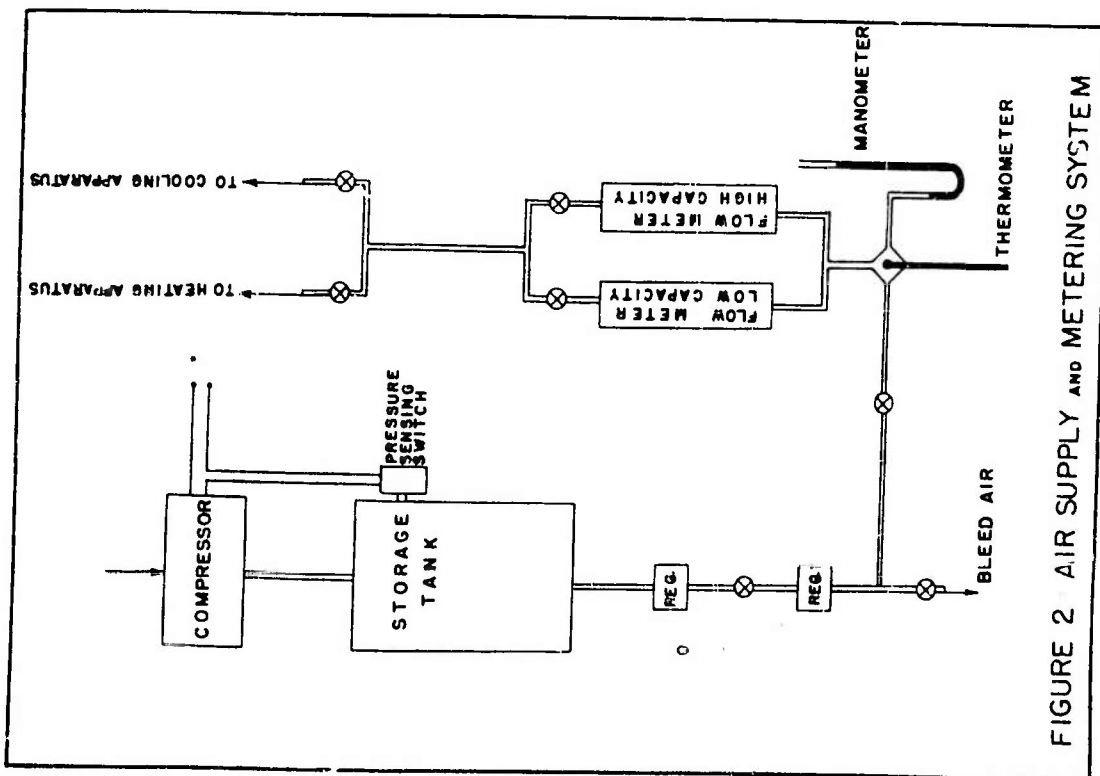
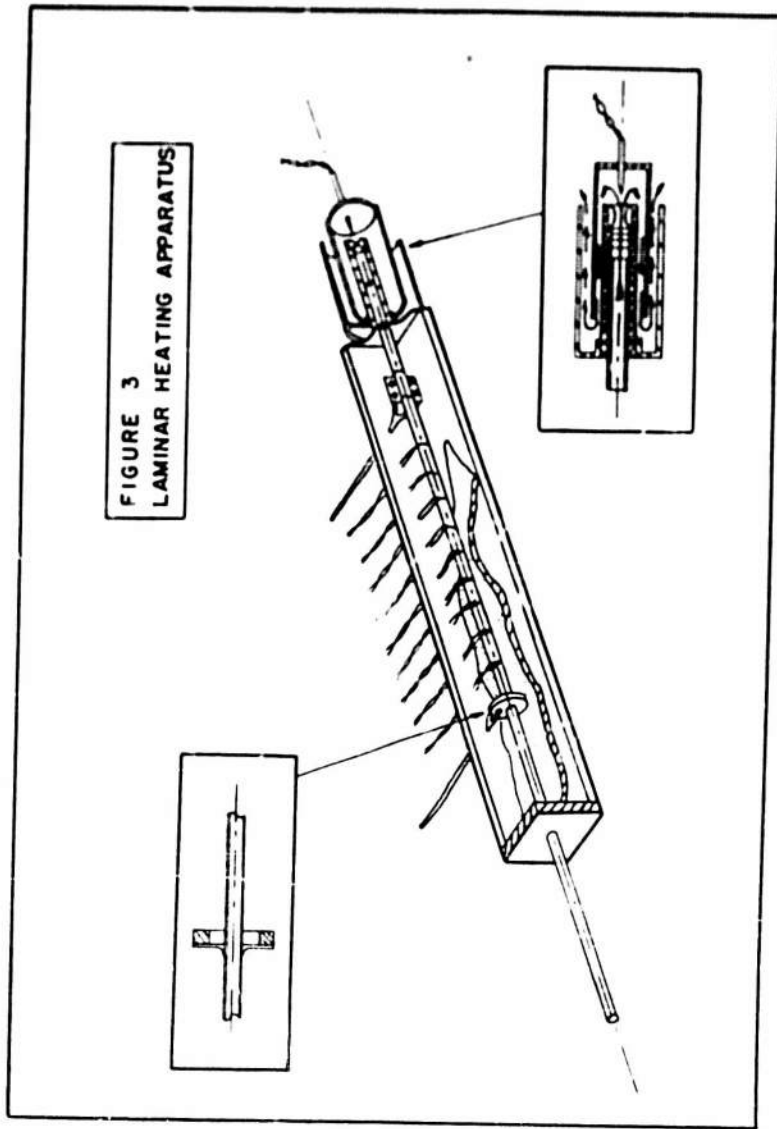
All the thermocouples used in this work are chromel-alumel. The thermocouples are connected to a zone box which has been thermally isolated by insulation, and in which copper plates have been placed to insure an isothermal zone. The zone box connects to a Leeds and Northrup 24-point thermocouple switch, and finally to a Leeds and Northrup Portable Precision Potentiometer.

A summary of the important dimensions of both the heating and cooling apparatus is given in Table I.

TABLE I
A SUMMARY OF IMPORTANT APPARATUS DIMENSIONS

Dimension	Gas Heating Apparatus	Gas Cooling Apparatus
Overall tube length	66"	62"
Tube inside diameter	0.375"	0.480"
Tube wall thickness	0.005"	0.010"
Entry length	30"	32"
Entry length L/D	80	66.7
Heat transfer section length	30"	30"
Heat transfer section L/D	80	62.5
Total heat transfer area	35.3 in ²	45.3 in ²

* Includes 6 inches extending beyond and at heating section.



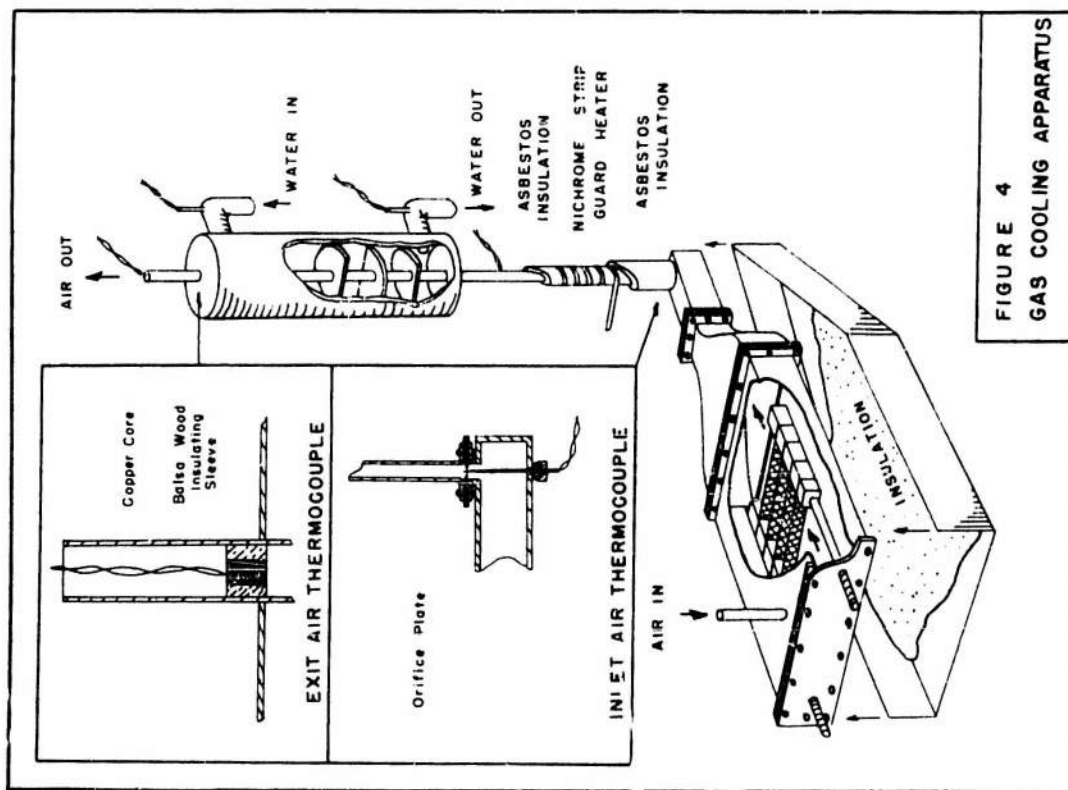


FIGURE 4
GAS COOLING APPARATUS

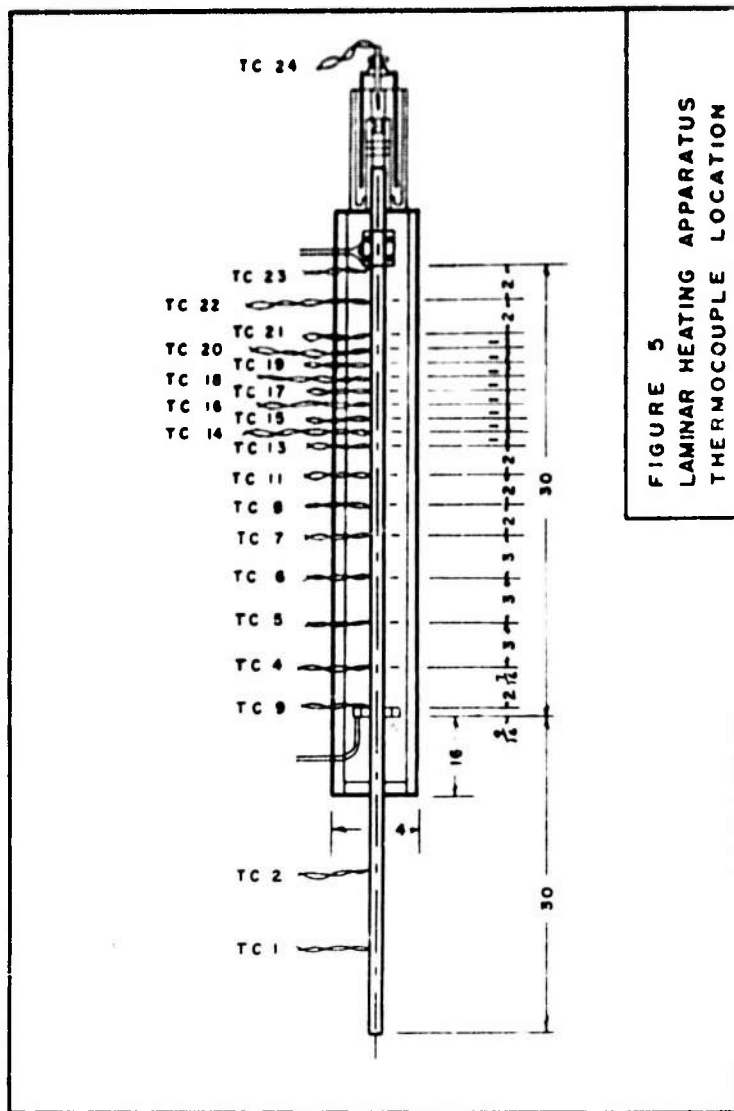


FIGURE 5
LAMINAR HEATING APPARATUS
THERMOCOUPLE LOCATION

SECTION V

REDUCTION OF EXPERIMENTAL DATA AND TEST RESULTS

Laminar Heating Experiments -- In the laminar flow heating experiments the measured quantities were the tube-wall temperature as a function of axial position, the air flow rate, the inlet air temperature, and the total power input. With this information, and knowledge of the magnitude of the heat losses through the surrounding insulation, the local heat transfer rates and local Nusselt numbers can be calculated.

Before describing the actual calculation procedure, the problem of heat losses through the insulation should be discussed. With the very low air flow rates involved, on the order of 1.3 pounds per hour, this problem was a very serious one. Actually the magnitude of the heat transfer through the insulation was of the same order as that to the air flowing inside the nichrome tube. Increasing the amount of insulation would have helped very little, in view of the already small tube-diameter-to-insulation-diameter ratio. The advantage of the small decrease in heat losses obtained in this way would have been more than compensated for by the increase in apparatus response time which would accompany any such solution.

Since it is necessary, in order to calculate the local Nusselt number, to have accurate knowledge of the local heat input, it was necessary to know the magnitude of the local heat losses accurately. For this reason a number of test runs were performed with no air flowing. From the measured axial distribution of wall temperature and the total power input, it was possible to construct a chart giving the local heat loss as a function of local wall-temperature-to-ambient-temperature difference and position.

The question may arise as to whether or not the local heat losses obtained in this way are the same as those which occur during the actual test runs, in view of the fact that

the axial temperature distributions were different. As long as the major share of the thermal resistance is in the insulation, and as long as the first derivative of the temperature versus axial position curve is small, the local heat losses as obtained previously should correspond to the losses under the actual test conditions. These conditions are least well satisfied in the entry to and the exit from the test section. Consequently the results from these regions contain greater uncertainty than do the results from other regions of the test section. Because of the possible error in the exit region, the calculations were not carried into this region. Calculations for the great bulk of the test section excluding this exit region, using the axial test run temperature distributions, indicate that the conditions enumerated above are adequately satisfied and that the use of the heat loss data obtained under conditions of no air flow introduces negligible error in the final result.

With heat loss as a function of axial position and temperature determined, the calculation procedure is as follows. Using the measured wall temperature distribution, the local heat loss as a function of position is determined.

$$L = L(x) \quad (16)$$

From the power input measurements and the local heat loss the local rate of heat transfer to the air flowing inside the tube can be found. Thus,

$$q' = P(x) - L(x) = q'(x) \quad (17)$$

Check calculations indicate that for Runs 1 to 4 inclusive the local power input can be assumed to be the same as the average power input over the length of the test section. Excluding the first 2 inches of the test section where the uncertainty due to the uncertainty in $L(x)$ is high, the effect of this assumption is to change the calculated N_{Nu} result by less than 1 per cent. For these runs

$$P(x) = P$$

Having now the heat transfer rate to the air inside the tube as a function of position, the local mixed mean air temperature can be determined. This is obtained by a simple energy balance on the volume included within the tube from the start of the heating section to the local point of interest. The resulting equation is

$$T_m = T_o + \frac{1}{wc_p} \int_0^x q' dx \quad (18)$$

It is now possible to calculate the local surface conductance. From the defining equation for the surface conductance

$$h = q'' / (T_w - T_m) \quad (19)$$

The rate of heat transfer per unit area is given by

$$q'' = q' / 2\pi r_o \quad (20)$$

Substituting Eqs. (20) and (18) into (19) gives

$$h(x) = \frac{P - L(x)}{2\pi r_o} \bigg/ \left[T_w - T_o - \frac{1}{wc_p} \int_0^x q' dx \right] \quad (21)$$

The local Nusselt number can then be determined from

$$N_{Nu} = hD/k \quad (22)$$

Actually the calculation procedure was somewhat more complex due to the fact that the air properties which entered into the above calculations for $h(x)$ are themselves functions of temperature. In effect, a local mean temperature was first assumed and used to evaluate a mean c_p for the range from T_o to T_m . Using this value of c_p a new mean temperature could be calculated. The mean c_p from T_o to T_m was then evaluated using the calculated value of T_m . This iteration procedure was followed until no significant change resulted.

All air properties used in these calculations were taken

from the National Bureau of Standards Bulletin No. 564.¹¹

In runs 5 and 6 the variation in tube electrical resistance makes the assumption of constant power input untenable, and the N_{Nu} calculated using this assumption must be corrected as follows:

$$N_{Nu} = \frac{hD}{k} = \frac{q'}{k\pi\Delta T}$$

Since k is not a function of the electrical resistance, R ,

$$\frac{dN_{Nu}}{N_{Nu}} = \frac{dq'}{q'} - \frac{d\Delta T}{\Delta T}$$

If, as is the case here, $\Delta q' \ll q'$ and $\Delta\Delta T \ll \Delta T$

$$\frac{\Delta N_{Nu}}{N_{Nu}} = \frac{\Delta q'}{q'} - \frac{\Delta\Delta T}{\Delta T}$$

where $\Delta q'$ and $\Delta\Delta T$ are the changes in q' and ΔT due to the variation of tube resistance, and where q' and ΔT are the values computed previously. Then,

$$P(x) = I^2 R(x)$$

Thus

$$\Delta P' = I^2 \Delta R(x)$$

where $\Delta R(x)$ is given by

$$\Delta R(x) = R\alpha\delta t$$

where α is the temperature coefficient of resistance of the tube, R is the length mean resistance, and where

$$\delta t = T_w(x) - \frac{1}{L} \int_0^L T_w(x) dx$$

Thus the actual power input is given by

$$\begin{aligned} \bar{P}(x) &= I^2 R + I^2 \Delta R \\ &= I^2 R \left(1 + \frac{\Delta R}{R}\right) \end{aligned}$$

$$\bar{P}(x) = P(x)[1 + \alpha\delta t]$$

where a bar over a quantity is used to indicate its corrected value.

Thus

$$\bar{q}' = \bar{P}(x) - L(x)$$

$$\bar{q}' = P(x)[1 + \alpha\delta t] - L(x)$$

$\Delta q'$ is easily found by subtracting \bar{q}' from the value of q' calculated previously.

$\Delta\Delta T$ can be found as follows:

$$\bar{\Delta T} = T_w - T_o - \frac{1}{wc_p} \int_0^x \bar{q}' dx$$

or

$$\bar{\Delta T} = T_w - T_o - \frac{1}{wc_p} \Sigma \bar{q}' \Delta L$$

Thus

$$\Delta\Delta T = \bar{\Delta T} - \Delta T$$

$$T = -\Sigma \frac{\bar{q}' \Delta L}{wc_p} + \Sigma \frac{q' \Delta L}{wc_p} = \frac{1}{wc_p} [\Sigma \bar{q}' \Delta L - \Sigma q' \Delta L]$$

The Nusselt numbers obtained above were plotted against a nondimensional distance x^+ , defined earlier. As x^+ involves the properties of the air, the question again arises as to where these properties should be evaluated. It was found that use of the local mixed-mean temperature brought about the best agreement between the experimental and the theoretical results.

As is well known, the analytical solutions for the local Nusselt number are dependent on the distribution of heat input. Since the local heat input in all the runs was very closely approximated by a step plus a ramp (negative), that is

$$q'' \cong q_o [1 + bL] \quad (23)$$

the results of a calculation for this type of heat input should apply to all the runs. It should be noted, however, that in general the value of b was different for different

runs. From general solution for variable heat input
(see Section II)

$$T - T_o = \frac{r_o}{k} \int_0^{x^+} g(x^+ - L, r^+) q(L) dL$$

or for $r^+ = 1$

$$T_w - T_o = \frac{r_o}{k} \int_0^{x^+} g(x^+ - L, 1) q(L) dL$$

Substituting for $g(x^+ - L, 1)$

$$T_w - T_o = \frac{r_o}{k} \int_0^{x^+} \left[4 - \sum_m \frac{e^{-\gamma_m^2(x^+ - L)}}{\gamma_m^2 H'_1(-\gamma_m^2)} \right] q(L) dL$$

For a step-plus-a-ramp type heat input,

$$q(L) = q_o''(1 + bL)$$

Substituting,

$$T_w - T_o = q_o'' \frac{r_o}{k} \int_0^{x^+} \left[4 - \sum_m \frac{e^{-\gamma_m^2(x^+ - L)}}{\gamma_m^2 H'_1(-\gamma_m^2)} \right] [1 + bL] dL$$

Integrating between the given limits,

$$T_w - T_o = q_o'' \frac{r_o}{k} \left\{ 4 \left[x^+ + \frac{bx^{+2}}{2} \right] + \sum \frac{e^{-\gamma_m^2 x^+}}{\gamma_m^4 H'_1(-\gamma_m^2)} - \sum_m \frac{1}{\gamma_m^4 H'_1(\gamma_m^2)} \right. \\ \left. - b \sum_m \frac{e^{-\gamma_m^2 x^+}}{\gamma_m^2 H'_1(-\gamma_m^2)} \left[e^{\gamma_m^2 x^+} \left(\frac{x^+}{\gamma_m} - \frac{1}{\gamma_m} \right) + \frac{1}{\gamma_m} \right] \right\}$$

Also, from energy considerations,

$$T_m - T_o = \frac{4r_o}{k} \int_0^{x^+} q''(x^+) dx^+$$

$$T_m - T_o = \frac{4r_o}{k} q_o'' \int_0^{x^+} (1 + bx^+) dx^+$$

$$T_m - T_o = \frac{4r_o}{k} q_o'' \left[x^+ + \frac{bx^{+2}}{2} \right]$$

Combining yields

$$T_w - T_m = q'' \frac{r_o}{k} \left\{ \sum_m \frac{e^{-\gamma_m^2 x^+}}{\gamma_m^4 H'(-\gamma_m^2)} - \sum_n \frac{1}{\gamma_m^4 H'(-\gamma_m^2)} \right. \\ \left. - b \sum_m \frac{e^{-\gamma_m^2 x^+}}{\gamma_m^2 H'(-\gamma_m^2)} \left[e^{\gamma_m^2 x^+} \left(\frac{x^+}{\gamma_m^2} - \frac{1}{\gamma_m} \right) + \frac{1}{\gamma_m} \right] \right\}$$

Since $N_{Nu_x} = hD/k$

$$N_{Nu_x} = \frac{q''}{T_w - T_m} \frac{2r_o}{k}$$

or

$$\frac{1}{N_{Nu_x}} = \frac{(T_w - T_m) k}{q''(1 + bx^+)} \frac{1}{r_o}$$

$$\frac{1}{N_{Nu_x}} = \left(\frac{1}{2} \right) \frac{1}{1 + bx} + \left\{ \sum_m \frac{e^{-\gamma_m^2 x^+}}{\gamma_m^4 H'(-\gamma_m^2)} - \sum_m \frac{1}{\gamma_m^4 H'(-\gamma_m^2)} \right. \\ \left. - b \sum_m \frac{1}{\gamma_m^2 H'(-\gamma_m^2)} \left[\frac{x^+}{\gamma_m^2} - \frac{1}{\gamma_m} + \frac{e^{-\gamma_m^2 x^+}}{\gamma_m} \right] \right\}$$

Simplifying further

$$-\sum_m \frac{1}{\gamma_m^4 H'(-\gamma_m^2)} = 32 \sum_n \frac{G_n}{\lambda_n^4}$$

From the arbitrary heat input solution,

$$32 \sum_n \frac{G_n}{\lambda_n^4} = \frac{11}{24}$$

Therefore,

$$-\sum_m \frac{1}{\gamma_m^4 H'(-\gamma_m^2)} = \frac{11}{24}$$

Therefore,

$$\frac{1}{N_{Nu_x}} = \frac{1}{2} \frac{1}{1 + bx^+} \left\{ \sum_m \frac{e^{-\gamma_m^2 x^+}}{\gamma_m^4 H'(-\gamma_m^2)} + \frac{11}{24} - b \sum_m \frac{1}{\gamma_m^2 H'(-\gamma_m^2)} \left[\frac{x^+}{\gamma_m^2} - \frac{1}{\gamma_m} + \frac{e^{-\gamma_m^2 x^+}}{\gamma_m} \right] \right\}$$

Define

$$A(x^+) = \sum_m \frac{e^{-\gamma_m^2 x^+}}{\gamma_m^4 H'(-\gamma_m^2)} + \frac{11}{24} \quad (24)$$

$$B(x^+) = \sum_m \frac{1}{\gamma_m^2 H'(-\gamma_m^2)} \left[\frac{x^+}{\gamma_m^2} + \frac{e^{-\gamma_m^2 x^+} - 1}{\gamma_m} \right] \quad (25)$$

Then

$$1/N_{Nu_x} = \frac{1}{2} \frac{1}{1 + bx^+} \left\{ A(x^+) - bB(x^+) \right\}$$

or

$$N_{Nu_x} = \frac{2(1 + bx^+)}{A(x^+) - bB(x^+)} \quad (26)$$

Values of $A(x^+)$ and $B(x^+)$ have been evaluated and are given in Table II.

TABLE II
THE FUNCTIONS $A(x^+)$ AND $-B(x^+)$

x^+	$A(x^+)$	$-B(x^+) \times 10^3$
0.02	.3232	4.919
0.04	.3843	12.09
0.06	.4156	20.14
0.08	.4329	28.61
0.10	.4431	37.36
0.12	.4492	46.52
0.14	.4529	56.26
0.16	.4551	64.55

The values of b used in Eq. (26) are found from the heat input given by Eq. (23).

Cooling Experiments -- In the cooling experiments, the local Nusselt numbers were not determined; only the length-mean Nusselt numbers were calculated. The experimental data taken consisted of the air flow rate, several temperatures along the entry length, the water inlet and outlet temperature, the air exit temperature, and the water flow rate.

Again the evaluation of both the experimental value of the Nusselt number and the theoretical solutions involve the problem of what temperature to use when evaluating the properties. Since the data is for the length-mean Nusselt number, it is necessary to use some sort of length-mean temperature. If the thermal transport properties are constant, and if the surface conductance (h) is constant, the length-mean temperature is the simple log-mean temperature which is usually employed in heat exchanger work. In the actual situation, however, this is not a true length-mean temperature for two reasons. First, the thermal conductivity is not constant; actually k is larger at the front part of the

cooling section where the air is at a higher temperature; and secondly, since the thermal boundary layer is not fully developed at the entrance to the cooling section, the Nusselt number there is considerably higher than at the exit.

In the case of the turbulent data the mean temperature was taken to be the simple log-mean temperature, as this is by far the easiest and since the entry length effect is small.

In the laminar case the data was reduced three times; once with the properties evaluated at the simple log-mean temperature, once with the properties evaluated at the exit temperature, and once with the properties evaluated at a mean temperature calculated from a Graetz solution which assumes constant properties but not fully developed thermal boundary layer. The evaluation at the log-mean temperature was done primarily for general interest and also to demonstrate the sensitivity of the results to the choice of temperature at which the properties are evaluated. The actual length-mean temperature will lie between the length-mean temperature given by the Graetz solution and the exit temperature, for the reasons discussed previously. Hence the effects of the radial variation of properties should lie between the effect indicated when the properties are evaluated at the Graetz solution mean temperature and the effect indicated when the properties are evaluated at the exit temperature.

The actual data reduction procedure for the turbulent data was as follows: Since the water temperature was constant within a few degrees, the log-mean temperature can be calculated from

$$T_m = T_w + \frac{\Delta T_{in} - \Delta T_{out}}{\ln \Delta T_{in} / \Delta T_{out}} \quad (27)$$

The effectiveness can be evaluated from

$$\epsilon = \frac{T_{h_{in}} - T_{h_{out}}}{T_{h_{in}} - T_{c_{out}}} \quad (28)$$

The NTU can be evaluated from

$$\epsilon = \frac{1 - e^{-NTU[1-(C_{\min}/C_{\max})]}}{1 - \frac{C_{\min}}{C_{\max}} e^{-NTU[1-(C_{\min}/C_{\max})]}} \quad (29)$$

which, in the case of very small C_{\min}/C_{\max} reduces to

$$\epsilon = 1 - e^{-NTU} \quad (30)$$

The average overall thermal conductance can be calculated from

$$NTU = \frac{AU_{ave}}{C_{\min}} \quad (31)$$

The surface conductance on the air side can be obtained from

$$\frac{1}{UA} = \frac{1}{h_{air}A_{inside}} + \frac{1}{h_{H_2O}A_{outside}} + \frac{t}{k} \quad (32)$$

where h_{H_2O} is obtained from¹³

$$\left[\frac{1}{0.6} \right] \left[\frac{h_{H_2O}}{k_{H_2O}} \right] = 0.33(N_{Pr})^{1/3}(N_{Re})^{0.6}(2r_o) \quad (33)$$

Except in the initial runs where the water flow rate was kept low so as to have a significant water temperature change with which to make an energy balance for check purposes, the thermal resistance of the water side was negligible, i.e., less than 1 per cent of the total.

The length-mean Nusselt number can then be evaluated from

$$N_{Nu} = hD/k \quad (22)$$

where k is evaluated at the log-mean temperature calculated above. The Reynolds number can be obtained from

$$N_{Re} = DG/\mu \quad (54)$$

where μ is evaluated at the log-mean temperature. The results were then normalized by dividing the experimental Nusselt number by the Nusselt number given by the solution of Sieder and Tietz using the N_{Re} obtained above to evaluate the exit x^+ .

For constant wall temperature the length-mean N_{Nu} is given by

$$N_{Nu_{iso}} = \frac{1}{2x^+} \ln \left[\frac{1}{8 \sum \frac{G_n}{\lambda_n^2} e^{-\lambda_n^2 x^+}} \right]$$

This N_{Nu} has been evaluated for various values of N_{Re} . For the apparatus in use x/r_0 is fixed. Assuming $N_{Pr} = \text{constant}$,

$$N_{Nu_{iso}} = \phi(N_{Re})$$

In the laminar case, using the log-mean temperatures, the data reduction procedure was the same, except of course, that the appropriate eigenvalues and constants from Appendix A were used for the calculation of $N_{Nu_{iso}}$.

For the second method of reduction, where the properties were evaluated at the mean temperature given by a Graetz solution, the calculation procedure was somewhat more complex. First the log-mean temperature was evaluated as above, and also an exit x^+ . From the Graetz solution a nondimensional mean temperature can be obtained as a function of the exit x^+ (see below). This new mean temperature is used to evaluate a new exit x^+ , and the procedure repeated until the value of the mean temperature is stable. A Nusselt number based on the properties at this temperature is then obtained. This Nusselt number is then normalized by dividing it by the mean Nusselt number $N_{Nu_{iso}}$ predicted by the Graetz solution for the final value of x^+ .

A mean temperature based on the Graetz solution can be

obtained as follows: From Eq. (7) the local mixed-mean temperature at any x^+ is given by

$$\theta_m = \frac{3}{\lambda_n^2} \sum_n \frac{G_n}{\lambda_n^2} e^{-\lambda_n^2 x^+}$$

The length-mean temperature is given by

$$\bar{\theta}_m = \frac{1}{x^+} \int_0^{x^+} \theta_m dx^+$$

Substituting and integrating yields

$$\bar{\theta}_m = -\frac{3}{x^+} \sum_n \frac{G_n e^{-\lambda_n^2 x^+}}{\lambda_n^4} - \frac{G_n}{\lambda_n^2} \quad (35)$$

Analysis of Experimental Uncertainty -- An analysis of the experimental uncertainty is presented in Appendix C. It is concluded that, employing the above described methods of reduction of data, the uncertainty in the measured Nusselt numbers for the laminar heating experiments is approximately ± 11 per cent. For the laminar cooling experiments an uncertainty of ± 5 per cent in Nusselt number is estimated, and for the turbulent cooling experiments the uncertainty in Nusselt number is estimated at $\pm 6\frac{1}{2}$ per cent.

Test Results -- The complete experimental data for laminar heating, laminar cooling, and turbulent cooling are presented in tabular form in Appendix B.

The laminar heating experiments consist of a series of six test runs each with an entering Reynolds number near 1200. Data were then recorded at a number of positions along the tube. It will be noted that the local Reynolds number decreases along the tube because of the increase of viscosity, this effect being most marked for the high temperature runs. Each run represents a successively higher heating rate with wall surface temperature reaching 1100°F for Run 6,

and the surface-to-fluid temperature difference reaching 570°F .

The laminar cooling experiments consist of a series of test runs at varying Reynolds numbers with the air inlet temperature successively increased to a maximum of 875°F .

The turbulent cooling experiments cover a Reynolds number range from about 13000 to 35000, with air inlet temperature varying up to a maximum of 1400°F .

The test results are presented graphically on Figs. 6 to 17. The laminar heating data are shown on Figs. 6 to 11 where the local Nusselt number is plotted as a function of the nondimensional length parameter, x^+ . On Fig. 12 the ratio of local measured Nusselt number to predicted Nusselt number is plotted as a function of the absolute wall-to-mean-fluid temperature ratio. The laminar cooling data are similarly plotted on Figs. 13, 14, and 15, using the three methods of evaluating fluid properties described previously. The turbulent cooling data are shown on Figs. 16 and 17. On Fig. 16 the measured overall mean Nusselt numbers are plotted as a function of Reynolds number. On Fig. 17 the ratio of Nusselt number to the Nusselt number predicted by the Sleicher and Tribus solution is plotted as a function of the temperature ratio.

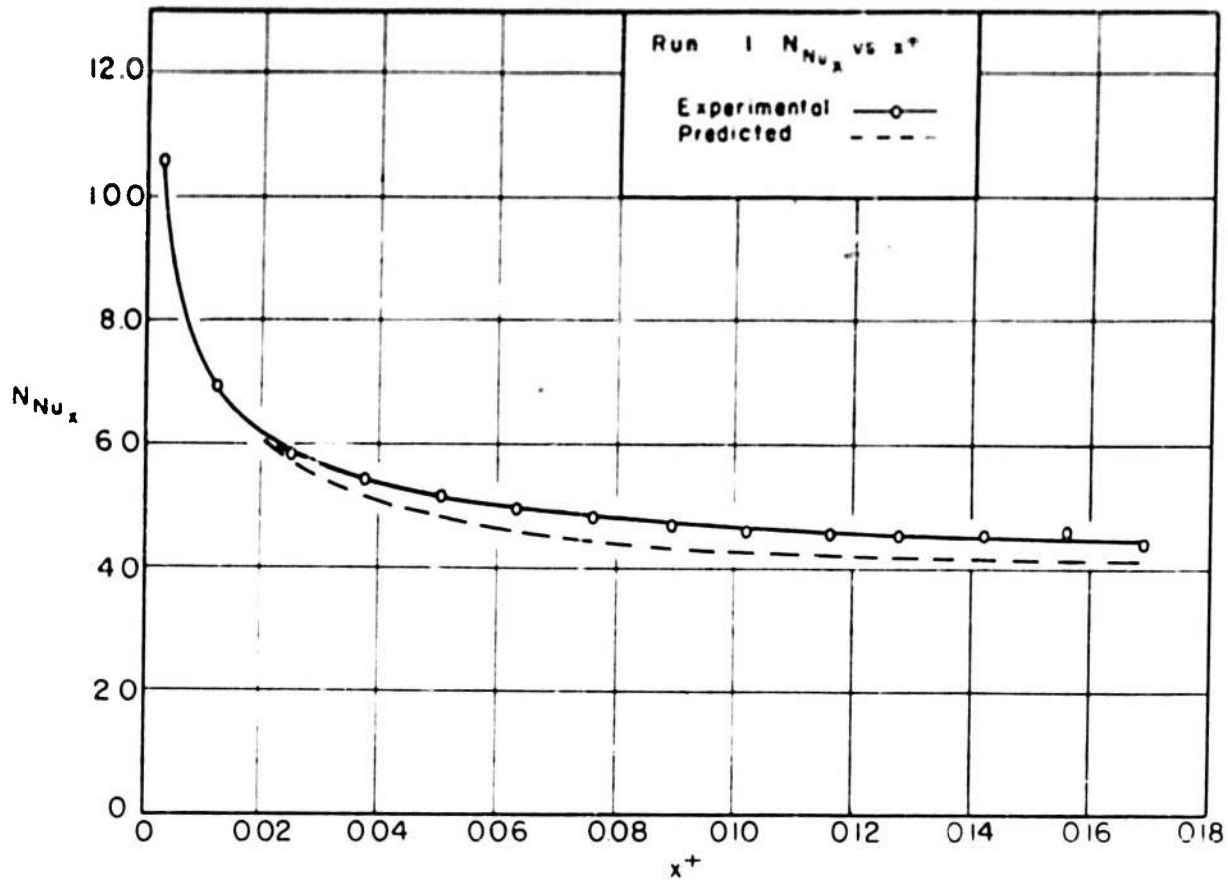


FIG 6. LAMINAR FLOW HEATING N_{Nu_x} vs x^+

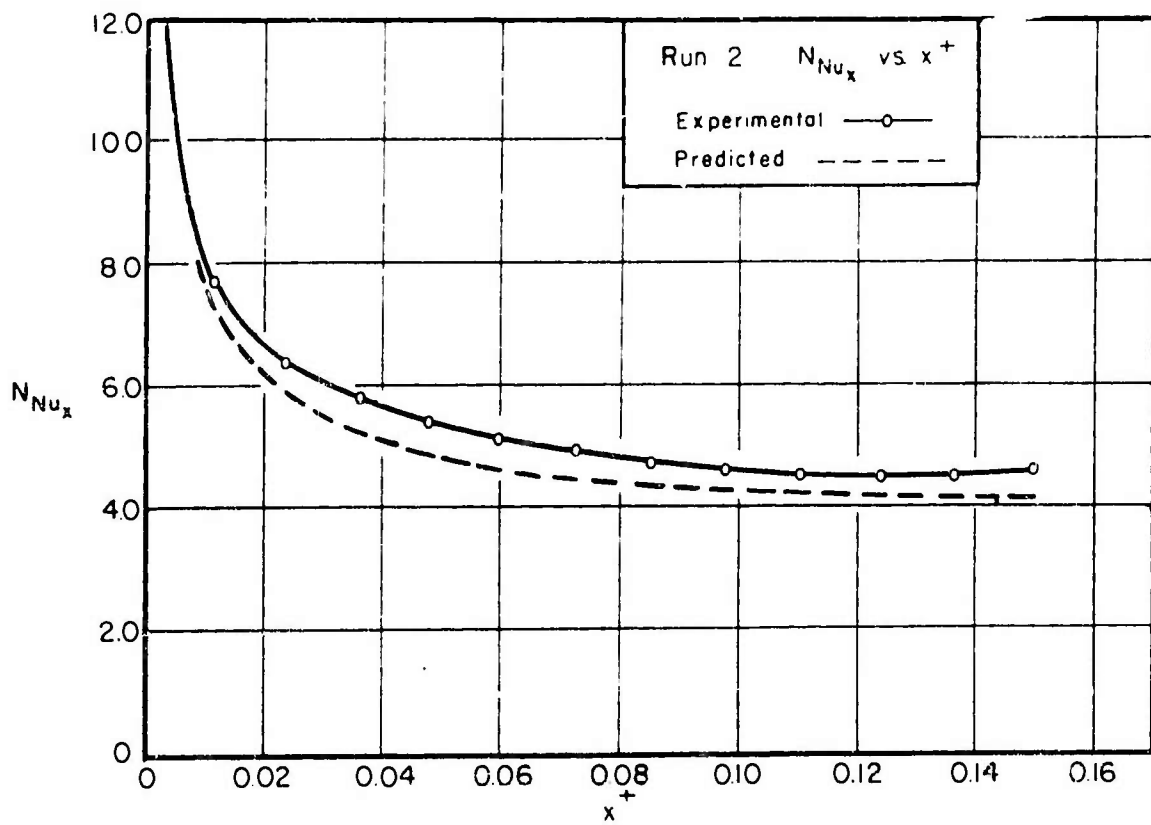


FIG 7. LAMINAR FLOW HEATING N_{Nu_x} vs x^+

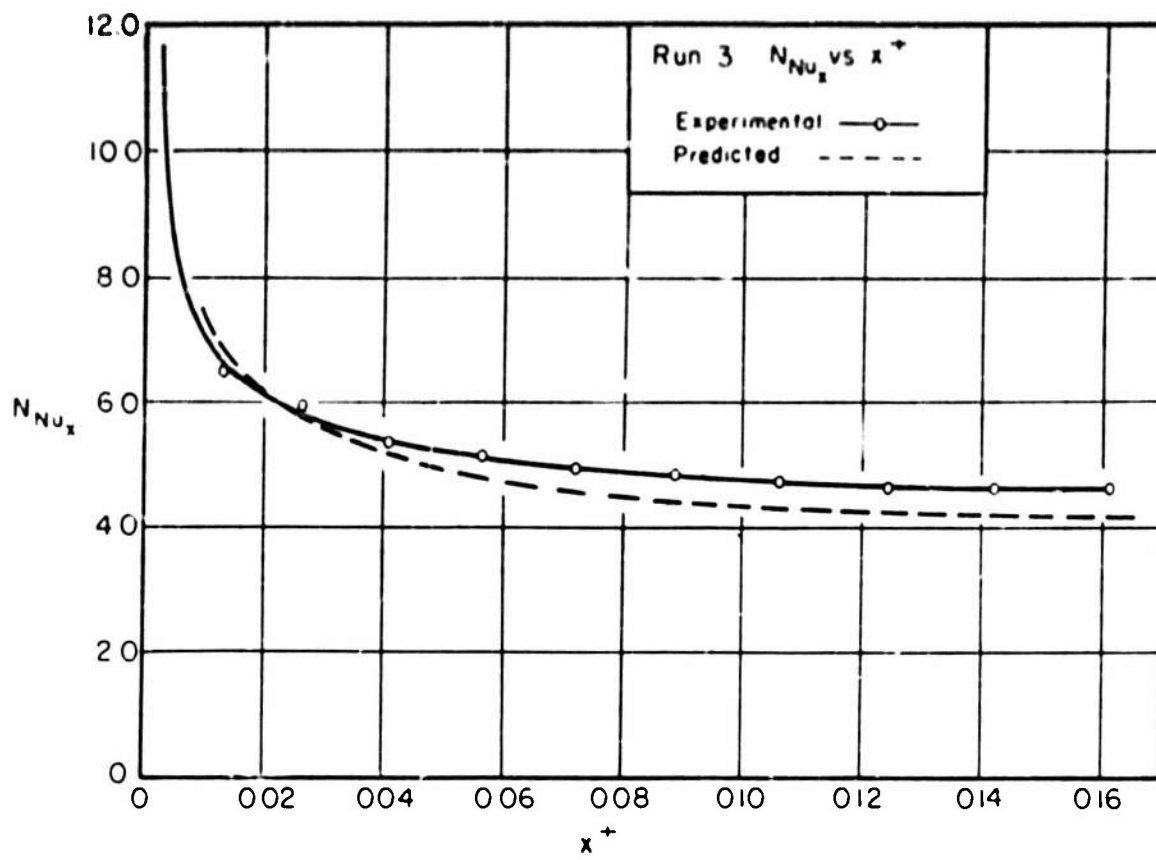


FIG 8. LAMINAR FLOW HEATING N_{Nu_x} vs x^+

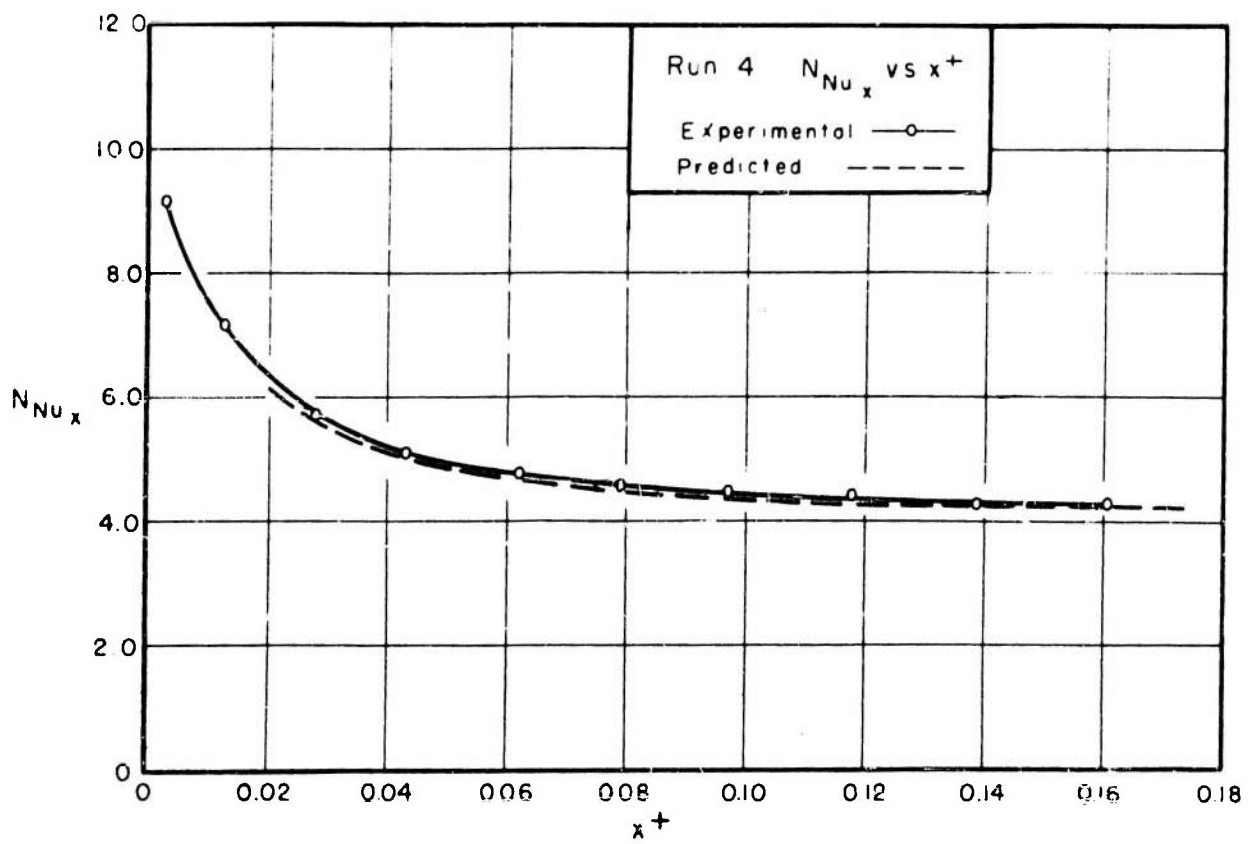


FIG 9. LAMINAR FLOW HEATING N_{Nu_x} vs x^+

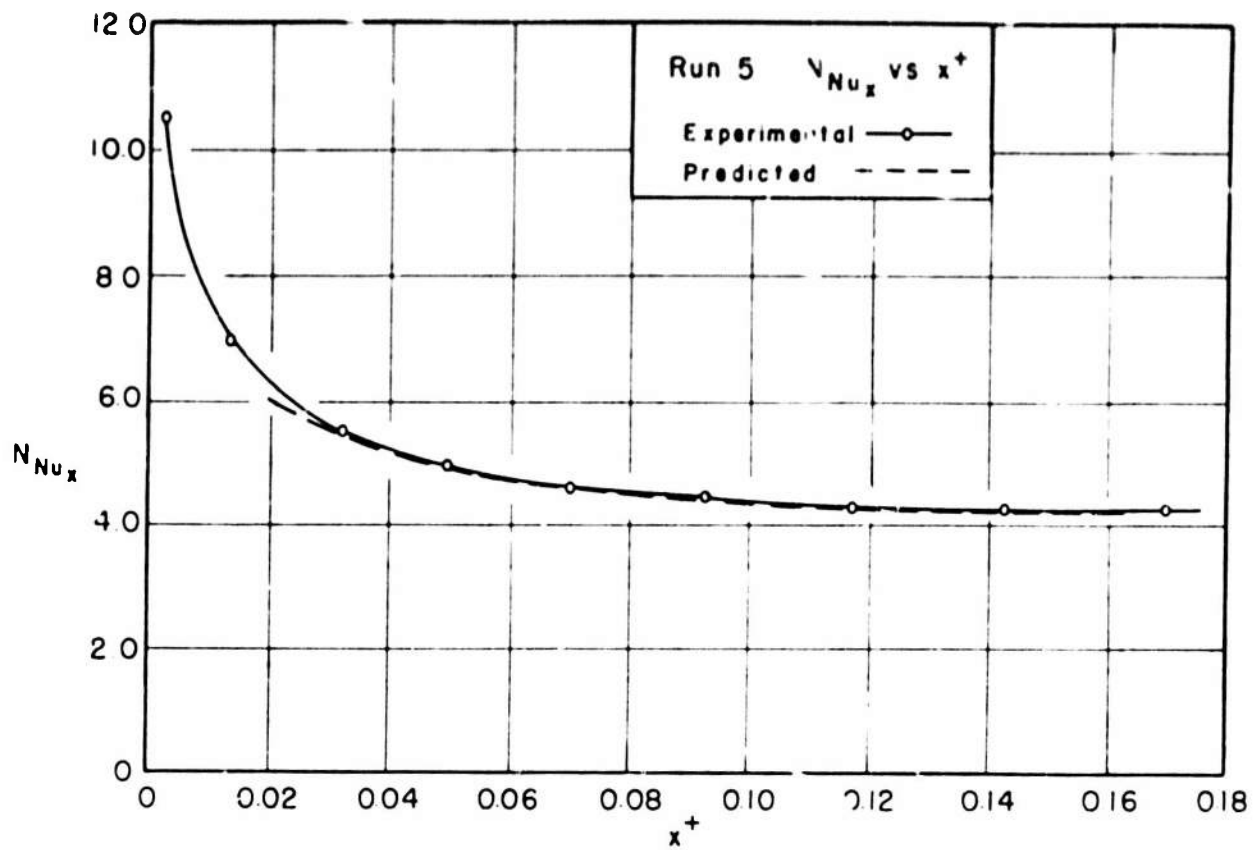


FIG 10 LAMINAR FLOW HEATING N_{Nu_x} vs x^+

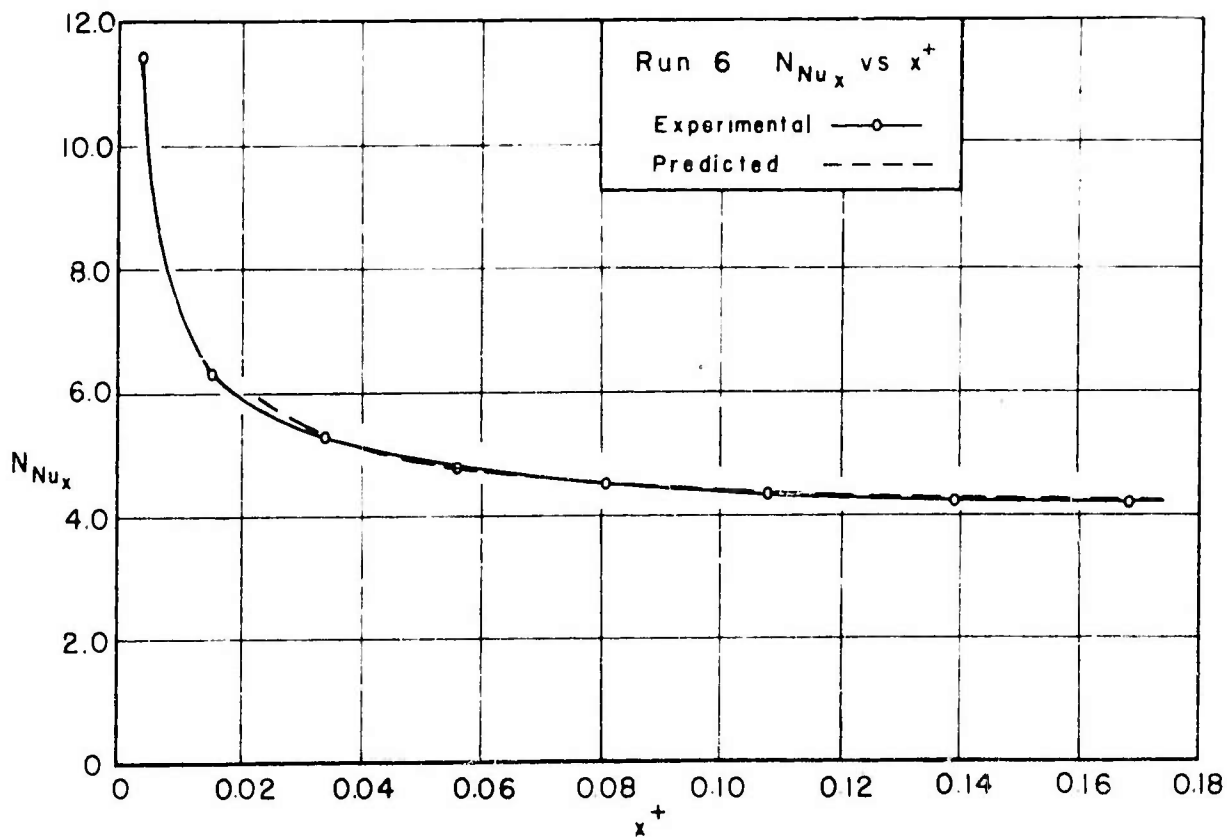


FIG 11 LAMINAR FLOW HEATING N_{Nu_x} vs x^+

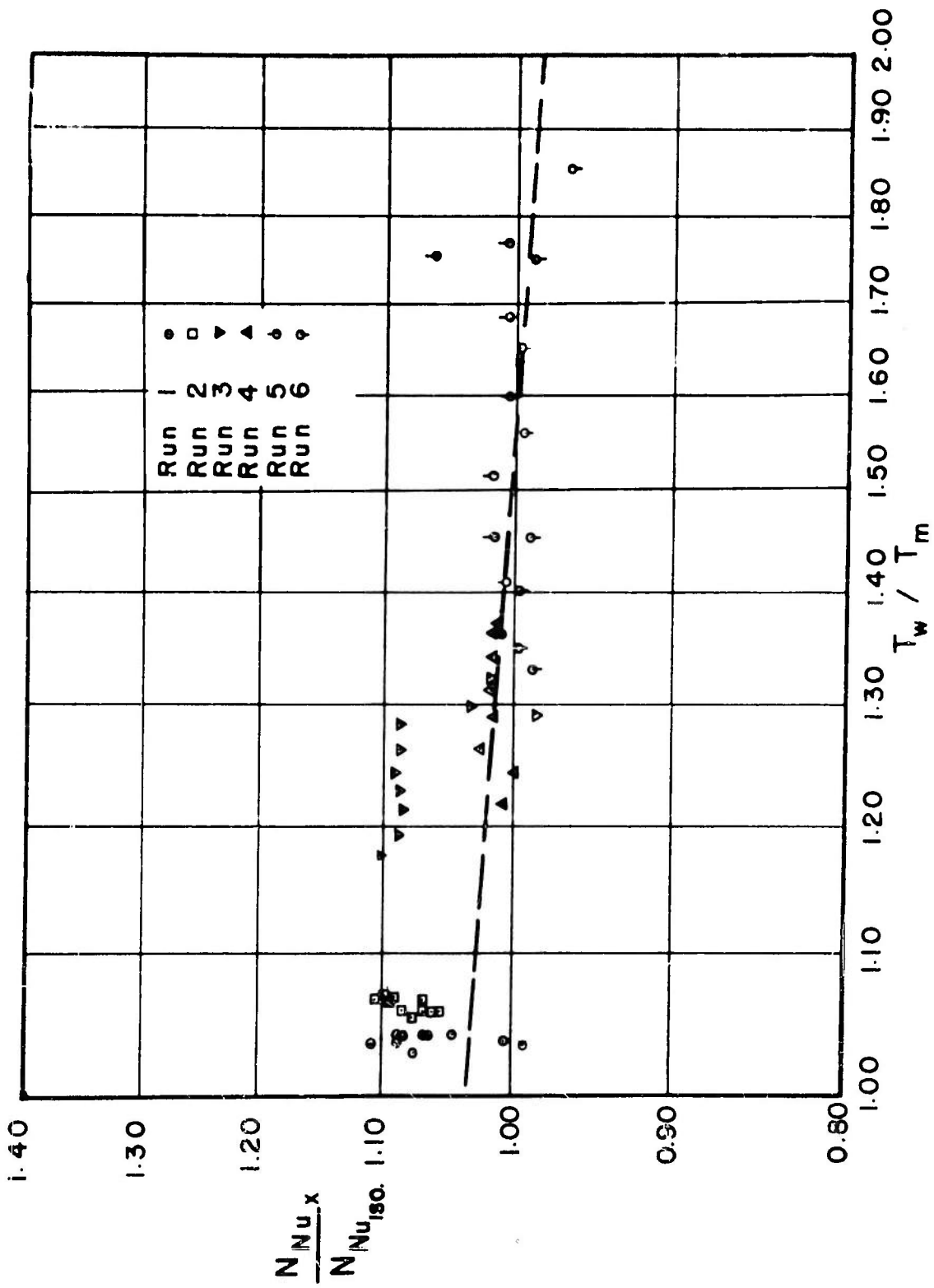


FIG 12. LAMINAR FLOW HEATING $N_{Nu_x} / N_{Nu_{iso}}$ vs T_w / T_m

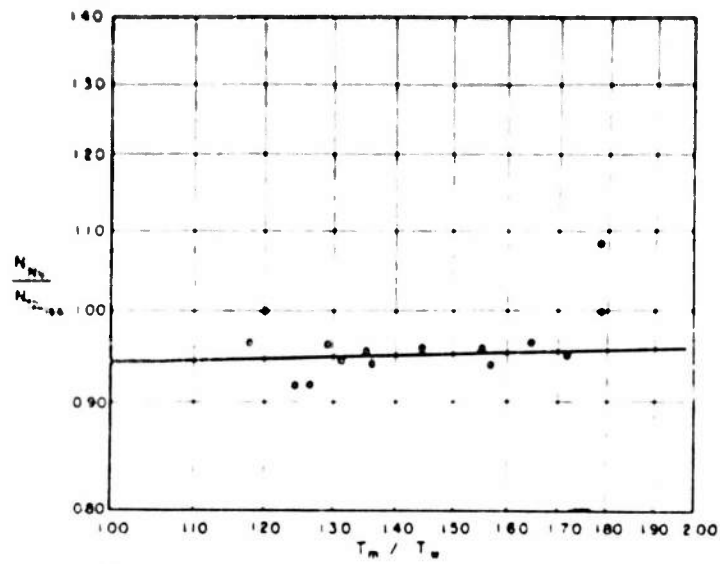


FIG 13 LAMINAR COOLING $N_{Nu} / N_{Nu,150}$ vs T_m / T_w
 PROPERTIES EVALUATED AT LOG MEAN TEMPERATURE

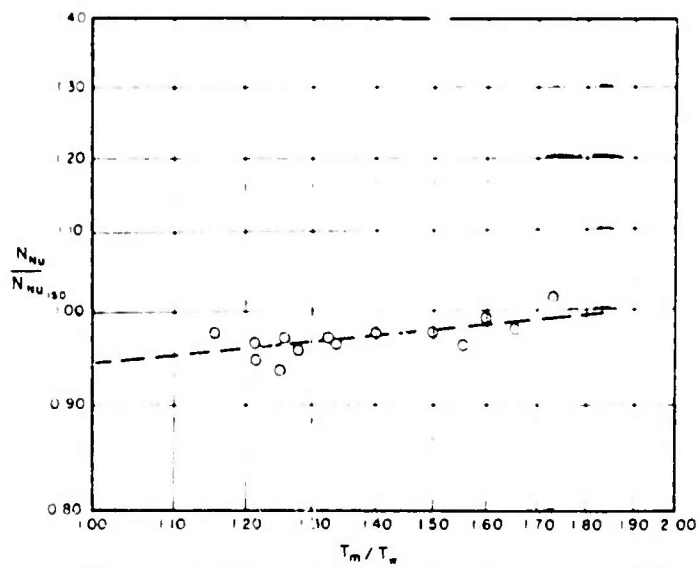


FIG 14 LAMINAR COOLING $N_{Nu} / N_{Nu,150}$ vs T_m / T_w
 PROPERTIES EVALUATED AT "GIAUQUE MEAN" TEMPERATURE

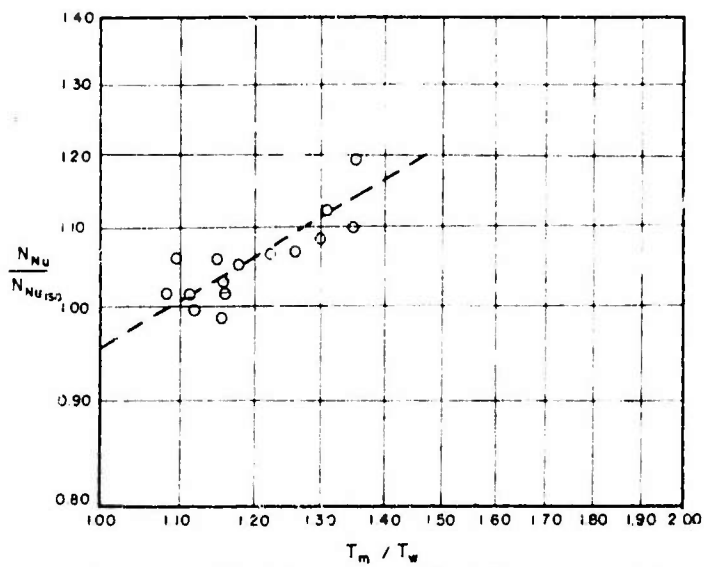


FIG 15 LAMINAR COOLING $N_{Nu} / N_{Nu,150}$ vs T_m / T_w
 PROPERTIES EVALUATED AT EXIT TEMPERATURE

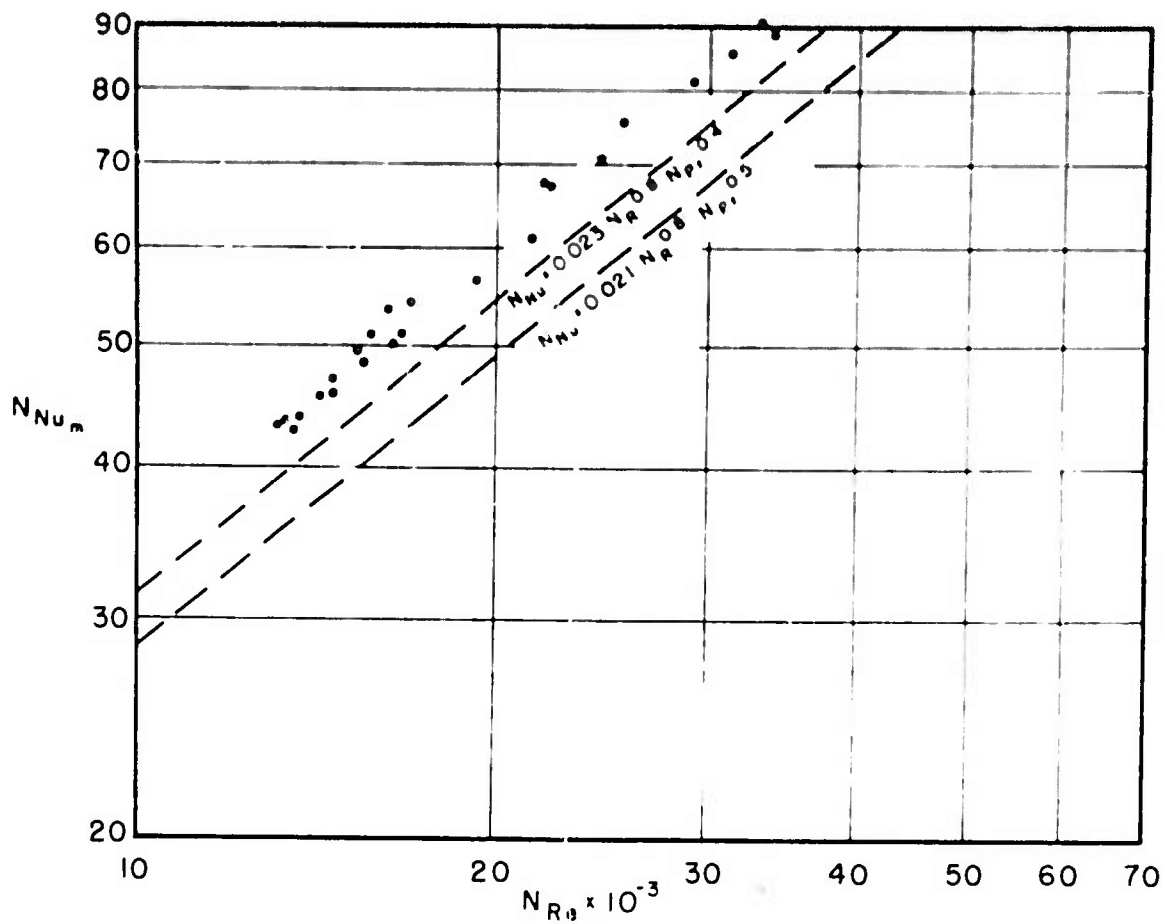


FIG 16 TURBULENT COOLING N_{Nu_m} vs N_{Re}

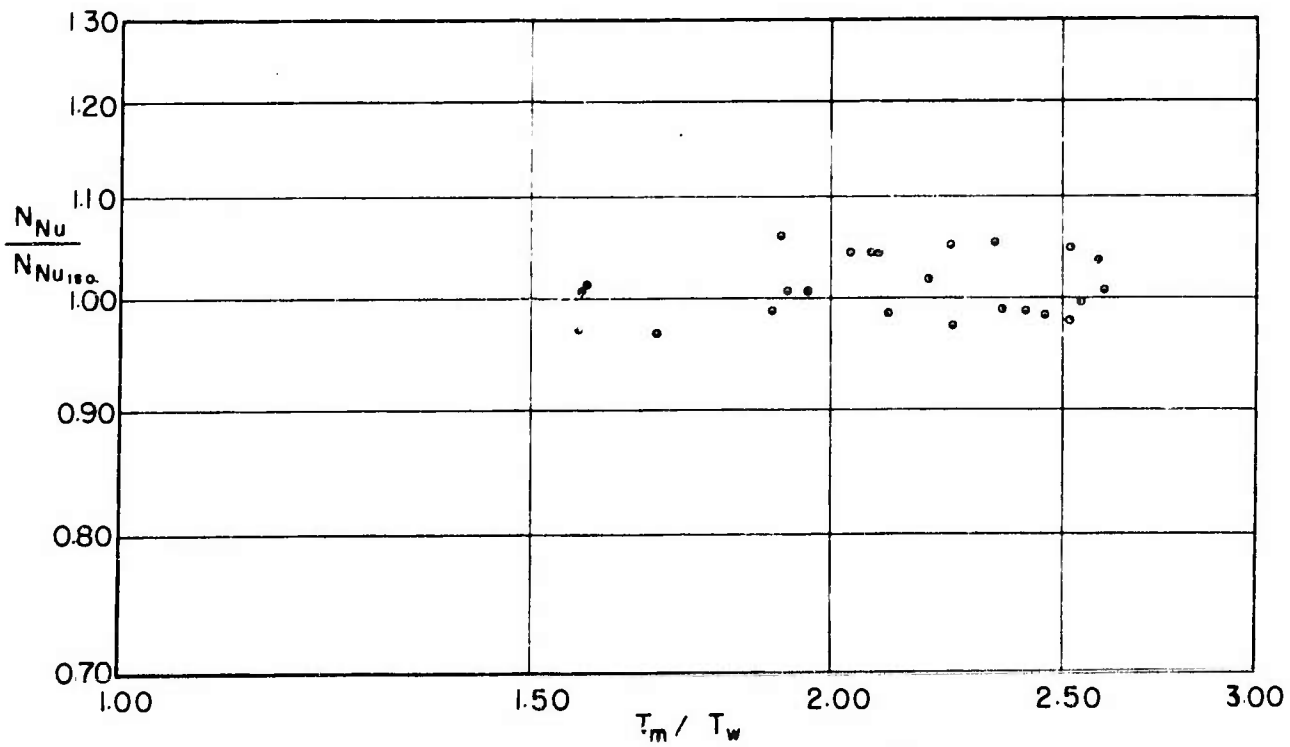


FIG 17 TURBULENT COOLING $\frac{N_{Nu}}{N_{Nu_{180}}}$ vs T_m / T_w

SECTION VI DISCUSSION OF TEST RESULTS

Laminar Heating -- The experimental values of the local N_{Nu} plotted against the local values of x^+ are shown in Figs. 6 to 11 inclusive. Also plotted as a dashed line are the values of the local N_{Nu} as predicted by the constant property analytical solutions for the actual heat rates which existed in each case.

It is seen that the experimental values correspond well to the theoretical solutions, even when the temperature differences involved are large and the thermal profile is developing. The agreement is actually best in the runs where the temperature differences involved were highest.

If there were an appreciable variable properties effect it should appear on a plot of $N_{Nu}/N_{Nu_{iso}}$ vs T_w/T_m , Fig. 12. The best straight line correlation indicates that the variable properties effect is negligible if the properties used in the evaluation of the local N_{Nu} are evaluated at the local mixed-mean temperature. Because of the scatter in the experimental data, and the rather large estimated experimental uncertainty, a small variable properties effect could be masked, but there is certainly no substantial effect, at least for temperature ratios up to 2.0. This is at variance with the analytical solutions which predict a drop in conductance for heating. However, the analytical solutions do not take into consideration any effects of the development of the temperature profile, or the effects of property variation with tube length, and it may well be that this is an effect that compensates for the influence of the distortion of the velocity and temperature profile at any particular cross-section.

Laminar Cooling -- The experimental values of $N_{Nu}/N_{Nu_{iso}}$ vs T_m/T_w for the laminar flow cooling experiments are shown in Figs. 13, 14, and 15. In Fig. 13 all properties were evaluated at the log-mean temperature. In Fig. 14 all

properties were evaluated at the mean temperature given by a Graetz solution, as discussed earlier. In Fig. 15 all properties were evaluated at the exit temperature.

In all these presentations the best straight line correlation intersects the Nu/Nu_{150} axis at about 0.94, indicating that the experimental results are about six per cent low. This is consistent with the estimated experimental uncertainty, and probably means that the major sources of uncertainty are fixed rather than random.

As was discussed in the section on data reduction, none of the temperatures used for the evaluation of the properties are the actual length-mean temperature. It is to be expected that the true length-mean temperature lies somewhere between the "Graetz mean temperature" and the exit temperature. Hence the true value of "a" should be somewhere between the value of the slope of the straight line correlation in Figs. 14 and 15. It is seen that Sze's predicted value of $a = -0.08$ does lie within this range. Hence, within the experimental uncertainty it would appear that Sze's prediction for the case of laminar cooling does apply. However, it should be noted that this is a quite small correction, and the important conclusion that one can draw is that both analysis and experiment are consistent in showing a small effect in the same direction.

In Fig. 13, where the properties were evaluated at the log-mean temperature, the temperature dependent properties effect appears to be negligible ($a = 0$). Thus it would appear that if the properties are evaluated at the log-mean temperature the variable properties effect could be ignored, in that it would be accounted for by evaluating the properties at the log-mean temperature. This is not entirely correct for the following reason. With the particular apparatus used for this work, the effects of property variation were just compensated by the error in evaluating the properties at the log-mean temperature. In general, however, if the geometry of the apparatus were changed one would not expect

this same result because it would then be possible to duplicate the same values of T_m/T_w (T_m = log-mean temperature) while altering the actual length-mean temperature and thus the variable properties effect. Again, however, since the effect is evidently small, it would seem that a satisfactory design procedure would be to evaluate all properties at log-mean temperature and ignore any effects of temperature dependent properties.

Turbulent Cooling -- The experimental values of N_{Nu} are shown as a function of N_{Re} in Fig. 16. It is seen that the data points are consistently above the values predicted by the commonly used fully developed turbulent flow correlations. This is partially due to the entrance effect; however, even if this is accounted for, the data points are still consistently about 10 to 20 per cent high. Experimental error might be suspected, if all other data was consistent with the common correlations. However, the experimental values of N_{Nu} correspond very well to the Sleicher and Tribus⁵ solution. Their solution in turn was based on their own experimental work. It is not known if any explanation for the discrepancy between the results of Sleicher and Tribus and the common correlations exists.

The experimental values of $N_{Nu}/N_{Nu_{iso}}$ (where $N_{Nu_{iso}}$ is the value predicted by Sleicher and Tribus) plotted against T_m/T_w are shown in Fig. 17. As can be seen, the data is best represented by $N_{Nu}/N_{Nu_{iso}} = 1.00$. Despite the discrepancy between the present data and the common correlations (or the discrepancy between the Sleicher and Tribus solution and the common correlations), it seems evident that there is negligible temperature dependent properties effect over the temperature ratio range 1.5 to 3.0, provided that all fluid properties are evaluated at the mean temperature with respect to length (the log-mean in this case).

SECTION VII

CONCLUSIONS

The conclusions of this investigation may be summarized as follows:

1. Two conclusions can be reached from the experimental data for laminar heating. The first is that the Graetz solution and its extensions seem to predict correctly the variation of local Nusselt number if the air properties are evaluated at the local mixed-mean temperature. That is to say, the thermal entry effect seems to correspond generally to that predicted by the proper analytical solution, even though the assumption of constant properties made in these solutions does not obtain. The second conclusion is that the actual effect of the radial variation of properties on the local Nusselt number is small, at least for temperature ratios up to 2.0. The best fitting straight line correlation (see Fig. 12) indicates that this effect is negligible provided all properties are evaluated at the local mixed-mean temperature. Because of the scatter in the experimental data and the rather large experimental uncertainty, a small property variation effect could be hidden, but certainly an effect as large as predicted does not seem to obtain.

2. For the cooling of a gas in laminar flow the data obtained were only for the mean Nusselt number with respect to tube length, rather than the local Nusselt number, but again the Graetz solution is apparently accurately applicable if all fluid properties are evaluated at a correct mean fluid temperature with respect to tube length. For constant wall temperature cooling, the logarithmic mean temperature is sufficiently close to the true mean, and in some cases is actually a better temperature at which to evaluate properties than the true mean. This conclusion is based on absolute-mean-temperature-to-wall-temperature ratios up to 2.0.

3. For a gas being cooled in turbulent flow, no

significant temperature dependent properties effects could be detected for absolute-mean-temperature-to-wall-temperature ratios from 1.5 to 3.0 . The experiments covered only mean Nusselt numbers with respect to tube length with constant wall temperature cooling, and all fluid properties were evaluated at the logarithmic mean, which for turbulent flow is very close to the actual mean temperature with respect to length.

This conclusion is in agreement with the experimental results of Zelnik and Churchill^{1,2}, who also found that the usual correlations hold for the case of turbulent cooling if all properties are evaluated at the mixed-mean temperature.

4. Consideration of the four significant regimes of heat transfer in a circular tube, laminar and turbulent flow, heating and cooling, leads to the conclusion that it is only in turbulent flow heating that there is a significant temperature dependent properties effect for gases, at least up to absolute temperature ratios of 2.0 or 3.0 . In all other cases the constant property analytical solutions, or the small temperature difference experimental correlations, are believed to be of acceptable accuracy for engineering calculations if all fluid properties are evaluated at the local mixed-mean temperature where local Nusselt numbers are concerned, and the mean temperature with respect to length in the case of mean Nusselt numbers. For turbulent flow heating the same procedure should be followed, with the exception that the resulting Nusselt number should be multiplied by $(T_w/T_m)^{0.5}$.

APPENDIX A

SUMMARY OF EIGENVALUES AND CONSTANTS

Laminar

$N_{Pr} = 0.7$, $N_R = 50,000$

n, m	λ_n^2	G_n	γ_m^2	$-H^1(-\gamma_m^2)$
0	7.512	0.740	-	-
1	44.62	0.544	25.68	7.650×10^{-5}
2	113.8	0.463	83.86	2.058
3	215.2	0.414	174.2	.01
4	343.5	0.382	295.6	.487
5	511.0	0.358	449.4	.297

n, m	λ_n^2	G_n	γ_m^2	$-H^1(-\gamma_m^2)$
0	235	28.6	-	-
1	2640	9.51	1.47	7.51×10^{-5}
2	7400	3.62	5230	1.97
3	(not compatible)		9875	.800
4	with m series)		15100	.402
5			23270	.228

$N_{Pr} = 0.7$, $N_R = 100,000$

0	400	40.0	-	-
1	4450	9.12	3557	4.12×10^{-5}
2	12800	5.66	9530	1.08
3	(not compatible)		17370	.443
4	with m series)		28940	.226
5			42230	.130

$N_{Pr} = 0.7$, $N_R = 500,000$

0	1470	176	-	-
1	16400	11.0	14300	$.942 \times 10^{-5}$
2	51000	17.2	39800	.244
3	(not compatible)		74700	.0998
4	with m series)		111500	.0508
5			174500	.0294

APPENDIX B

SUMMARY OF EXPERIMENTAL DATA

SUMMARY OF EXPERIMENTAL RESULTS
LAMINAR HEATING EXPERIMENTS

Run No.	Position in.	w lbs/hr	NRe	x ⁺	Total Heat Input Btu/in	Heat Loss Btu/in	q' Btu/in	t _w °F	t _w -t _o °F	t _m °F	t _w -t _m °F	$\frac{T_w}{T_m}$ °R/°R	NNu	NNu _{iso}	$\frac{N_{Nu}}{N_{Nu_{iso}}}$
1	2	1.32	1218	.0124	.846	.273	.572	90.6	24.9	69.6	21.0	1.040	6.92	7.00	.990
	4	"	1212	.0248	"	.305	.541	96.5	30.5	73.1	23.4	1.042	5.93	5.75	1.010
	6	"	1202	.0375	"	.328	.518	100.5	34.5	76.5	24.0	1.045	5.41	5.20	1.040
	8	"	1195	.0504	"	.351	.495	103.7	37.7	79.8	23.9	1.045	5.16	4.85	1.065
	10	"	1190	.0632	"	.374	.472	106.6	40.6	82.8	23.8	1.045	4.92	4.60	1.070
	12	"	1190	.0760	"	.390	.455	108.9	42.9	85.6	23.3	1.042	4.82	4.40	1.090
	14	"	1186	.0993	"	.411	.434	111.2	45.2	88.3	22.9	1.041	4.66	4.20	1.090
	16	"	1180	.1020	"	.429	.417	113.1	47.1	91.0	22.1	1.040	4.61	4.05	1.092
	18	"	1175	.1160	"	.444	.401	114.9	48.8	93.5	21.3	1.040	4.59	4.20	1.090
	20	"	1172	.1275	"	.460	.386	116.5	50.5	96.0	20.5	1.038	4.56	4.20	1.095
	22	"	1170	.1420	"	.475	.371	119.2	52.2	98.5	19.7	1.035	4.54	4.15	1.091
	24	"	1165	.1560	"	.495	.351	119.2	53.5	100.7	18.5	1.032	4.56	4.10	1.110
	26	"	1161	.1692	"	.523	.322	120.5	54.5	102.9	17.6	1.032	4.39	4.10	1.070
	2	2	1.41	1305	.0116	1.422	.444	.973	100.0	40.0	67.8	32.2	1.060	7.73	7.30
4		"	1300	.0231	"	.498	.925	103.5	49.5	73.3	36.2	1.070	6.44	6.00	1.070
6		"	1280	.0353	"	.517	.895	116.2	56.2	78.6	37.6	1.070	5.90	5.30	1.110
8		"	1270	.0475	"	.583	.839	122.0	62.0	83.8	38.2	1.070	5.44	4.92	1.100
10		"	1265	.0595	"	.620	.802	127.0	67.0	88.8	38.2	1.070	5.15	4.70	1.090
12		"	1255	.0721	"	.655	.767	131.2	71.2	93.4	37.8	1.070	4.94	4.50	1.096
14		"	1247	.0949	"	.686	.736	135.1	75.1	97.8	37.3	1.070	4.77	4.35	1.095
16		"	1238	.0975	"	.718	.701	138.6	78.6	102.0	36.6	1.065	4.62	4.30	1.070
18		"	1230	.1107	"	.749	.673	141.8	81.8	106.1	35.7	1.065	4.50	4.25	1.060
20		"	1220	.1240	"	.769	.653	144.0	84.0	110.0	34.0	1.060	4.55	4.20	1.092
22	"	1220	.1368	"	.794	.623	146.6	86.6	113.9	32.8	1.059	4.52	4.20	1.075	

SUMMARY OF EXPERIMENTAL RESULTS
LAMINAR HEATING EXPERIMENTS

Run No.	Position in.	w lbs/hr	N _{Re}	x ⁺	Total Heat Input Btu/in	Heat Loss Btu/lr	q' Btu/lr	t _w °F	t _w -t _o °F	t _m °F	t _w -t _m °F	$\frac{T_w}{T_m}$ °R/°R	N _{Nu}	N _{Nu} 150	$\frac{N_{Nu}}{N_{Nu}150}$
3	2	1.34	1185	.0128	5.768	1.917	3.851	227.0	160.8	92.0	145.0	1.29	6.49	9.65	.775
	4	"	1155	.0262	"	2.159	3.609	267.0	200.8	114.0	143.0	1.32	5.95	5.15	1.020
	6	"	1120	.0407	"	2.255	3.503	287.0	220.8	137.5	149.5	1.30	5.24	5.15	1.035
	8	"	1090	.0561	"	2.332	3.376	304.0	237.8	158.0	146.0	1.28	5.12	4.70	1.088
	10	"	1070	.0719	"	2.513	3.255	320.0	258.8	179.0	141.0	1.26	4.96	4.55	1.088
	12	"	1047	.0884	"	2.624	3.114	334.0	267.8	199.0	135.0	1.24	4.83	4.45	1.090
4	14	"	1022	.1060	"	2.750	3.018	348.0	281.8	217.5	130.5	1.23	4.74	4.35	1.088
	16	"	1002	.1204	"	2.879	2.899	360.0	293.8	236.0	124.0	1.21	4.67	4.20	1.082
	18	"	990	.1420	"	2.993	2.775	371.0	304.8	253.0	118.0	1.19	4.63	4.25	1.085
	20	"	970	.1610	"	3.101	2.657	381.0	314.8	271.0	110.0	1.18	4.67	4.20	1.100
	2	1.33	1175	.0129	9.200	3.032	6.168	310.0	244.3	103.0	207.0	1.37	7.15	7.00	1.018
	4	"	1100	.0276	"	3.419	5.781	371.0	305.3	141.0	230.0	1.39	5.70	5.65	1.005
	6	"	1060	.0435	"	3.687	5.513	408.0	342.3	175.0	232.0	1.36	5.13	5.01	1.020
	8	"	1020	.0621	"	3.910	5.290	437.0	371.3	210.0	227.0	1.34	4.52	4.70	1.020
	10	"	985	.0790	"	4.114	5.086	462.0	395.3	243.0	219.0	1.31	4.82	4.70	1.020
	12	"	957	.0978	"	4.283	4.902	483.0	417.3	274.0	209.0	1.29	4.51	4.40	1.020
	14	"	930	.115	"	4.450	4.750	502.0	436.3	305.0	197.0	1.26	4.49	4.30	1.036
	16	"	907	.139	"	4.710	4.490	523.0	457.3	334.0	184.0	1.24	4.26	4.25	1.000
18	"	895	.161	"	4.957	4.311	538.0	472.3	362.0	175.0	1.22	4.26	4.25	1.038	

SUMMARY OF EXPERIMENTAL RESULTS
LAMINAR HEATING EXPERIMENTS

Run No.	Position	w In.	N _{Re}	x ⁺	Total Heat Input Btu/in	Heat Loss Btu/in	q'	t _w	t _w -t _o	t _m	t _w -t _m	$\frac{T_w - T_m}{T_m} \frac{Pr}{Nu}$	N _{Nu}	N _{Nu,iso}	$\frac{N_{Nu}}{N_{Nu,iso}}$
5	2	1.32	1110	.0137	17.14	5.939	11.301	500	430.3	140	360	1.75	6.98	9.50	1.01
	4	"	1013	.0320	"	6.491	10.649	600	530.3	202	392	1.79	5.52	5.43	1.02
	6	"	956	.0491	"	6.895	10.115	662	582.3	273	391	1.84	4.93	4.90	1.01
	8	"	801	.0700	"	7.395	9.755	708	538.3	337	371	1.60	4.85	1.60	1.01
	10	"	958	.0925	"	7.678	9.502	748	678.3	337	351	1.53	4.50	4.41	1.02
	12	"	814	.117	"	8.029	8.111	791	714.3	151	330	1.66	4.39	4.30	1.02
6	2	"	785	.143	"	9.366	8.774	820	750.3	310	310	1.41	4.32	4.28	1.01
	4	"	758	.169	"	8.758	8.482	850	780.3	561	289	1.36	4.28	4.22	1.02
	6	1.30	1020	.0152	27.51	10.21	17.30	750	676.0	142	558	1.87	8.30	9.55	.863
	8	"	924	.0335	"	10.71	16.90	970	746.0	300	571	1.77	5.29	5.35	.990
	10	"	850	.0559	"	11.34	15.17	446	972.0	403	543	1.65	4.84	4.80	.998
	12	"	787	.0810	"	11.91	14.60	1015	941.0	500	515	1.56	4.54	4.55	.993
7	2	"	738	.108	"	12.41	15.10	1075	1001.0	595	480	1.47	4.37	4.40	.995
	4	"	688	.114	"	13.01	14.50	1132	1058.0	696	445	1.40	4.29	4.30	.997
	6	"	664	.168	"	13.52	13.99	1182	1103.0	772	410	1.35	4.24	4.25	.998

SUMMARY OF EXPERIMENTAL RESULTS

TURBULENT COOLING EXPERIMENTS

Run No.	w lbs/hr	t _w °F	t _{in} °F	t _{exit} °F	NTU	t _m °F	N _{Re}	N _{Nu}	N _{Nu iso} (Sleicher and Tribus)	$\frac{N_{Nu}}{N_{Nu iso}}$	$\frac{T_m}{T_w}$ °R/°F
1	40.7	62.1	1400	530	1.049	893	15,220	49.7	43.2	1.03	2.59
2	35.4	63.3	1485	508	1.159	905	13,130	43.7	43.3	1.01	2.61
3	35.7	65.0	1433	499	1.147	883	13,410	44.0	44.0	1.00	2.55
4	35.6	65.0	1394	494	1.120	861	13,570	43.2	44.2	.980	2.51
5	40.7	63.0	1350	499	1.085	851	15,600	51.6	49.2	1.05	2.51
6	35.6	65.0	1344	479	1.117	832	13,730	43.7	44.5	.982	2.46
7	36.0	65.0	1303	469	1.120	909	14,010	45.0	45.3	.995	2.42
8	35.6	65.0	1224	474	1.120	762	14,550	46.2	46.5	.995	2.38
9	40.8	61.7	1218	456	1.084	771	16,280	53.4	50.2	1.06	2.36
10	35.4	65.0	1148	420	1.115	720	14,550	45.4	46.5	.975	2.25
11	40.8	62.6	1139	431	1.070	725	16,700	53.8	51.8	1.06	2.26
12	40.8	63.0	1082	412	1.075	690	17,010	53.9	52.6	1.02	2.20
13	36.0	66.0	1032	384	1.110	650	15,470	48.2	49.0	.984	2.12
14	59.8	70.0	994	397	1.035	618	25,600	76.0	73.0	1.04	2.09
15	50.8	67.0	921	379	1.003	608	22,300	68.3	65.5	1.04	2.03
16	50.8	67.0	956	398	1.015	628	22,090	67.7	65.0	1.04	2.07
17	69.8	67.5	863	365	.991	574	31,200	84.7	84.0	1.01	1.96
18	54.1	71.0	856	353	1.025	564	24,500	71.2	70.6	1.01	1.92
19	35.6	67.8	835	328	1.110	537	16,400	50.6	51.1	.990	1.89
20	71.6	68.0	811	348	.975	542	32,980	92.9	87.6	1.07	1.90
21	56.0	68.5	504	247	.979	373	29,100	81.3	80.0	1.02	1.88
22	43.1	69.5	535	238	1.020	432	21,410	61.1	63.5	.962	1.89
23	65.2	68.3	532	249	.944	369	33,850	89.7	89.0	1.01	1.57
24	36.3	68.5	530	231	1.040	353	19,190	56.2	58.0	.970	1.56

APPENDIX C
ANALYSIS OF EXPERIMENTAL UNCERTAINTY

Laminar Heating Experiments -- The uncertainty in the experimental determination of Nusselt number for the laminar heating experiments can be estimated by an analysis of the uncertainty of the various items of information going into Eqs. (21) and (22). It will be noted that the tube diameter cancels out and the pertinent variables are power measurement, heat leak, flow rate, the temperature difference between the tube wall and the entering fluid, and the fluid properties. Two test runs, representing extremes of the test data, have been analyzed, and the following tables list the magnitude and estimated probable uncertainty in the pertinent variables (neglecting the specific heat for which the probable uncertainty is small relative to the others).

Run No. 1, Position 20"

Variable	Magnitude	Uncertainty Interval	Relative Uncertainty
Gross Power, Btu/in	0.846	---	± 0.01
Heat Leak Btu/in	0.460	---	± 0.04
$(T_w - T_o), ^\circ F$	50.5	± 0.5	---
$\frac{1}{wc_p} \int_0^x q'dx, ^\circ F$	31.4	(computed)	---
w, lbs/hr	---	---	± 0.02
k, Btu/(hrft ² °F/ft)	---	---	± 0.02

Run No. 6, Position 14"

Variable	Magnitude	Unvertainty Interval	Relative Uncertainty
Gross Power, Btu/in	27.51	---	0.01
Heat Leak, Btu/in	13.52	---	0.04
$(T_w - T_o), ^\circ F$	1108	5.0	---
$\frac{1}{wc_p} \int_0^x q' dx, ^\circ F$	739°	(computed)	---
w, lbs/hr	---	---	0.02
k, Btu/(hrft ² °F/ft)	---	---	0.02

Employing the root-mean-square approximation for single sample experiment uncertainty estimation, the following probable relative uncertainty was computed for the Nusselt number determination.

Run No. 1	± 0.11
Run No. 6	± 0.11

Thus the uncertainty in the Nusselt number determination is estimated to be approximately ± 11 per cent for all of the test runs.

This rather large experimental uncertainty is in major part attributable to the large relative importance of the heat leak, and the ± 4 per cent uncertainty placed on the heat leak calibration. It is worth noting that of the six test runs, in only two do the measured Nusselt numbers differ by as much as 11 per cent from the theoretical constant property solution. It is thus felt that ± 11 per cent may be quite conservative. Furthermore, it is probable that the heat leak error is consistently in one direction rather than random, so that when comparing one test run with another

to detect effects of temperature dependent properties the uncertainty in the comparison would be substantially less than ± 11 per cent.

Laminar and Turbulent Cooling Experiments -- The major sources of uncertainty in the cooling experiments are in the measurement of the inlet and exit air temperatures, the air flow rates, and the uncertainty in the thermal conductivity of the air. The difficulty with the inlet temperature measurement was particularly significant. In order to satisfy the assumption of a fully established velocity profile it was necessary to have a velocity developing section after the inlet air temperature measurement. The developing section was wrapped with a nichrome ribbon guard heater, and a number of thermocouples were attached along the tube so that the guard heater could be adjusted to maintain the tube wall temperature the same as the inlet air temperature. It turned out to be difficult to maintain the entire tube at the same temperature, and the best that could be done was to make the temperature versus position pattern along the tube approximately similar for each run. In view of this difficulty it is estimated that the uncertainty interval in temperature difference between the inlet air and the cooling water is no better than ± 5 per cent. With this temperature difference reaching as high as 1400°F , the uncertainty interval is thus estimated as high as $\pm 70^{\circ}\text{F}$, which is approximately the kind of variation that was measured along the tube for the highest temperature runs. The uncertainty in the exit temperature is considerably less, and a ± 2 per cent estimate in the exit temperature difference is probably quite conservative. As in the laminar heating experiments, the uncertainty in flow rate and thermal conductivity is estimated at ± 2 per cent.

With these estimated uncertainties, the uncertainty in the resulting Nusselt numbers are calculated as follows using the root-mean-square approximation.

Laminar Cooling Experiments

Run No. 3 ± 0.048

Run No. 15 ± 0.045

Turbulent Cooling Experiments

Run No. 2 ± 0.055

Run No. 23 ± 0.064

It thus is concluded that for the laminar cooling experiments the uncertainty in the measured Nusselt numbers is approximately ± 5 per cent, and for the turbulent cooling experiments the uncertainty is approximately $\pm 6\frac{1}{2}$ per cent. These results are consistent with the scatter of the experimental points.

REFERENCES

1. Discussion by R. Lipkis, Trans. ASME, Vol. 77, 1955, pp. 1272-1273.
2. "Measurements of Average Heat Transfer and Friction Coefficients for Subsonic Flow of Air in Smooth Tubes at High Surface and Fluid Temperatures," by L. V. Humble, W. H. Lowdermilk, and L. G. Desmond, NACA Report 1020, 1951.
3. "Heat Transfer to Laminar Flow in a Round Tube or Flat Conduit - The Graetz Problem Extended," by J. R. Sellars, M. Tribus, and J. S. Klein, Trans. ASME, Vol. 78, 1956, pp. 441-448.
4. "Steady Laminar Heat Transfer in a Circular Tube With Prescribed Wall Heat Flux," by R. Siegel, E. M. Sparrow, and T. M. Hallman, Applied Scientific Research, Series A, Vol. 7, 1958, pp. 386-392.
5. "Heat Transfer in a Pipe With Turbulent Flow and Arbitrary Wall Temperature Distribution," by C. A. Sleicher, Jr., and M. Tribus, Heat Transfer and Fluid Mechanics Institute, 1956, pp. 59-79.
6. "Variation of Eddy Conductivity With Prandtl Modulus and its Use in Prediction of Turbulent Heat Transfer Coefficients," by R. Jenkins, Heat Transfer and Fluid Mechanics Institute, 1951, pp. 147-158.
7. "The Effect of Temperature-Dependent Fluid Properties on Heat Transfer and Flow Friction for Gas Flow," Ph.D. Dissertation by B. C. Sze, Department of Mechanical Engineering, Stanford University, Stanford, California, 1957.
8. "Turbulent Heat Transfer in the Thermal Entrance Region of a Pipe With Uniform Heat Flux," by E. M. Sparrow, T. M. Hallman, and R. Siegel, Applied Scientific Research, Series A, Vol. 7, pp. 37-52.
9. "The Influence of Non-Uniform Heat Flux on the Convection Conductances in a Nuclear Reactor," by W. M. Kays and W. B. Nicoll, TR-No. 33, Department of Mechanical Engineering, Stanford University, Stanford, California, November 1, 1957.
10. "Heat Transfer and Fluid Friction for Fully Developed Turbulent Flow of Air and Supercritical Water with Variable Fluid Properties," by R. G. Diessler, Trans. ASME, Vol. 76, Jan. 1954, pp. 73-85.

11. "Tables of Thermal Properties of Gases," U.S. Department of Commerce, National Bureau of Standards, Circular 564, Washington, D. C., November, 1955.
12. "Convective Heat Transfer from High Temperature Air Inside a Tube," by H. E. Zelinik and S. W. Churchill, ASME-AIChE Joint Heat Transfer Conference, State College, Pa., August, 1957.
13. "Heat Transmission," by W. H. McAdams, McGraw-Hill Book Company, New York, N.Y., 1954.

